UNIVERSITY OF THESSALY

SCHOOL OF ENGINEERING

DEPARTMENT OF MECHANICAL ENGINEERING

WEAKLY NONLINEAR ANALYSIS OF THE EFFECT OF SHELL STIFFNESS ON THE FUNDAMENTAL RESONANCE OF COATED MICROBUBBLES

by

SOTIRIS ROSIOS

Submitted in partial fulfillment of the requirements for the degree of Diploma in Mechanical Engineering at the University of Thessaly

Volos, 2021

UNIVERSITY OF THESSALY

SCHOOL OF ENGINEERING

DEPARTMENT OF MECHANICAL ENGINEERING

WEAKLY NONLINEAR ANALYSIS OF THE EFFECT OF SHELL STIFFNESS ON THE FUNDAMENTAL RESONANCE OF COATED MICROBUBBLES

by

SOTIRIS ROSIOS

Submitted in partial fulfillment of the requirements for the degree of Diploma in Mechanical Engineering at the University of Thessaly

Volos, 2021

Approved by the Committee on Final Examination:

Advisor	Prof. N. Pelekasis Department of Mechanical Engineering, University of Thessaly,
Member	Prof. K. Papadimitriou, Department of Mechanical Engineering, University of Thessaly
Member	Assistant Prof. G. Charalampous Department of Mechanical Engineering, University of Thessaly

Acknowledgements

I would like to express my sincere appreciation and gratitude to my supervisor Prf. Nikos Pelekasis for placing his trust and support in me until the completion of the present diploma thesis. His constant guidance and support were of the utmost importance and had a great impact in the quality of the thesis.

I would like to thank the members of the committee Prof. Kostas Papadimitriou and Assistant Prof. Georgios Charalampous for dedicating time to read an evaluate my thesis.

I would also like to thank my parents for their selfless support and encouragement, throughout the duration of my studies in the department of mechanical engineering. Nothing would have been possible without it.

WEAKLY NONLINEAR ANALYSIS OF THE EFFECT OF SHELL STIFFNESS ON THE FUNDAMENTAL RESONANCE OF COATED MICROBUBBLES

SOTIRIS ROSIOS

Department of Mechanical Engineering, University of Thessaly, 2021

Supervisor: Prof. Nikos Pelekasis

Computational Fluid Dynamics

Abstract

The nonlinear radial oscillations of a spherical gas bubble encapsulated in an elastic shell are investigated by means of an asymptotic method when the viscous forces and compressibility effects of the surrounding liquid are accounted for. The microbubble is immersed in an infinite, Newtonian surrounding fluid and subject to a sinusoidal acoustic excitation in the far field. Three different constitutive laws have been employed describing the viscoelastic properties of the shell, namely the Kelvin-Voight (KV), the Mooney-Rivlin and the Skalak (SK) models are used, pertaining to an almost linear for small displacements, strain-softening, and strain-hardening behavior of the material, respectively. Approximate analytical solutions describing the steady-state oscillations have been obtained, corresponding to the fundamental resonance of the bubble, that are valid to second order of approximation in terms of the sound amplitude. The obtained results are displayed in the form of frequency response curves of the steady-state solutions for different sets of parameters. When the membrane exhibits a strain-softening behavior the response curves shift to lower than the natural resonance frequencies whereas when the material behavior is described as strain-hardening the opposite results are obtained. . The results obtained analytically are compared to the ones obtained numerically in previous studies with satisfactory agreement, especially when weak damping mechanisms are considered.

Keywords: bubble oscillations, steady-state solution, encapsulated bubbles, compressibility effects, analytical solutions

WEAKLY NONLINEAR ANALYSIS OF THE EFFECT OF SHELL STIFFNESS ON THE FUNDAMENTAL RESONANCE OF COATED MICROBUBBLES

ΣΩΤΗΡΗΣ ΡΟΣΙΟΣ

Τμήμα Μηχανολόγων Μηχανικών, Πανεπιστήμιο Θεσσαλίας, 2021

Επιβλέπων Καθηγητής: Πελεκάσης Νίκος

Καθηγητής Υπολογιστικής Ρευστοδυναμικής

Abstract

Οι μη γραμμικές ταλαντώσεις σφαιρικής φυσαλίδας, περιβαλλόμενης από ελαστικό κέλυφος, που περιέχει αέριο, μελετώνται με τη χρήση ασυμπτωτικής ανάλυσης όταν οι ιξώδεις δυνάμεις και τα φαινόμενα συμπιεστότητας του ρευστού λαμβάνονται υπόψιν. Η φυσαλίδα είναι βυθισμένη σε Νευτώνειο ρευστό χωρίς παρουσία συνόρων και υποκείμενη σε ημιτονοειδή ακουστική διαταραχή. Τρεις διαφορετικοί καταστατικοί νόμοι χρησιμοποιήθηκαν για την περιγραφή των ιξωδοελαστικών ιδιοτήτων του κελύφους, ο νόμος Kelvin-Voight, ο νόμος Mooney-Rivlin και ο νόμος Skalak που αφορούν σε σχεδόν γραμμικά για μικρές μετατοπίσεις, strain-hardening και strain-softening υλικά αντίστοιχα. Προσεγγιστικές αναλυτικές λύσεις λήφθηκαν για τη μόνιμη κατάσταση της θεμελιώδους ταλάντωσης σε συνθήκες συντονισμού που είναι αποδεκτές στη δεύτερη τάξη προσέγγισης με βάση το πλάτος της ακουστικής διαταραχής. Τα αποτελέσματα αναπαρίστανται σε γραφήματα συναρτήσει της συχνότητας για τη μόνιμη κατάσταση για διαφορετικές τιμές των εμπλεκόμενων παραμέτρων. Όταν η μεμβράνη χαρακτηρίζεται ως strain-softening οι καμπύλες απόκρισης συντονισμού μετατοπίζονται σε συχνότητες χαμηλότερες της ιδιοσυχνότητας του συστήματος, ενώ η αντίθετη συμπεριφορά παρατηρείται για strain-hardening υλικά. Τα αποτελέσματα που λαμβάνονται από την προσεγγιστική αναλυτική λύση, συγκρίνονται με αποτελέσματα που λήφθηκαν μέσω αριθμητικών μεθόδων σε προηγούμενες μελέτες και παρατηρείται ικανοποιητική συμφωνία, ιδίως για μικρές τιμές των παραμέτρων που αφορούν στους μηχανισμούς απόσβεσης.

Λέξεις-Κλειδιά: ταλαντώσεις φυσαλίδας, λύση μόνιμης κατάστασης, ενθυλακωμένες φυσαλίδες, συμπιεστή ροή, αναλυτικές λύσεις

Contents

1 INTRODUCTION

The oscillating motion of a bubble, immersed in a viscous, slightly compressible liquid, insonated by an acoustic disturbance in the far field is investigated in the present study.

A bubble is capable of oscillating in a variety of ways. These oscillations are described by periodic variations in its shape and volume. It is possible that some of the oscillation modes occur simultaneously and a very complex resultant motion is produced. This motion can be even more difficult to describe and solve when the full parameters of the system bubble-host liquid are accounted for.

The most straight forward case is the one referring to a spherically symmetric gas bubble performing a purely radial motion surrounded in an incompressible fluid. When formulated, the system can be described by the Rayleigh-Plesset equation and when coupled with the appropriate kinematic and dynamic boundary conditions it yields the instantaneous radial position of the bubble surface.

Because of the highly nonlinear nature of the governing equations, the oscillations of a bubble in a liquid present a difficult mathematical problem. Attempted solutions are either numerical or analytical based on simplified versions of the initial nonlinear problem neglecting terms that in general contribute to the response of the investigated bubble. One of the first and more rigorous attempts to the full nonlinear problem was made by Prosperetti, (1974)[3] who studied the steady state of the bubble oscillations in an incompressible fluid analytically, using the Krylov-Bogolyubov asymptotic method. Lauterborn, (1974)[4] approached the same subject numerically and produced similar results. Samek, (1980)[5] attempted an analytical solution to the same subject using the Bogolyubov – Mitropolskiy asymptotic expansion technique. All authors mentioned studied the main, harmonic, and subharmonic resonances of the microbubble subject to an acoustic disturbance. Regarding the main resonance, which is the subject of the present study, they found the existence of a shift in the amplitude curves towards lower frequencies than the natural frequency of the bubble, indicating a “soft spring” behavior of the system while “jump” phenomena were observed in the numerical studies.

Moving on from the incompressible flow problem a more systematic approach led to various forms of the Rayleigh-Plesset equation accounting for compressibility effects. The most notable ones were listed by Prosperetti and Lezzi, (1986)[7] along with their version of the problem formulation. They showed that entire families of equations exist having the same degree of accuracy and therefore are entirely equivalent on formal ground. In the present study the equation used is the one developed by Keller and Miksis, (1980)[6] which includes the effects of acoustic radiation, compressibility, viscosity, surface tension and an incident sound wave.

Encapsulated microbubbles are investigated by adding shell thickness, elasticity, and viscosity terms to the normal stress balance for the bubble interface. In the earlier attempts, the membrane was modeled in a linear way with a constant elasticity. Church, (1995)[8] in his study derived a variation of the Rayleigh-Plesset equation describing the dynamics of encapsulated gas bubbles. He modeled the shell of the bubble as continuous layers of incompressible solid elastic material. In his derivations the finite thickness of the shell was considered and a double interface for the bubble wall was produced. He extracted analytical solutions of the derived equations for the fundamental and second harmonic response and concluded that the resonance frequency of individual bubbles increase as the modulus of rigidity increases, while the damping of the system is dictated by viscous terms. Frinking and De Jong, (1998)[9] studied microbubbles encapsulated in thicker membranes and modeled the shell as a viscoelastic solid. They used linear models or semiempirical laws for the shell elasticity and viscosity respectively and obtained numerical solutions to an altered Rayleigh-Plesset equation. They developed a model that described the linear and nonlinear responses of the encapsulated bubbles and underlined the effects of the shell on the response of the bubble. Khismatullin and Nadim, (2002)[11] undertook a more rigorous mathematical approach towards the description of the radial pulsations of encapsulated bubbles. They derived an equation describing linearly pulsating microbubbles using the method of matched asymptotic expansions.

The Kelvin-Voight and the 4-constant Oldroyd model were employed to describe the viscoelastic properties of the shell and the liquid respectively and the acoustic disturbance was restricted to small values. They showed that if the bubble is small and covered by a membrane whose thickness is much smaller than the bubble radius, the damping mechanism of the radial oscillations is governed by the shell viscosity. Moreover, when the surrounding liquid is viscoelastic, its viscous damping contributions are much smaller to those of a Newtonian liquid. It was also shown that the resonance frequency of an encapsulated bubble highly depends on the liquid and shell viscosities and thus it differs from the undamped natural frequency and resonance occurs at higher frequencies for the encapsulated bubbles.

Most materials though do not respond to external stresses in a linear way. The Kelvin-Voight model does not account for changes in the material induced by the external stresses applied on it. Unlike the linear stress-strain behavior predicted by Hooke's law, most materials exhibit a varying apparent elasticity modulus when they are subject to external disturbances of increasing intensity or increasing frequency []. Materials whose slope increases as deformations extend are called strain-hardening while materials with a decreasing slope are called strain-softening. Barthes-Biesel et al. (2002)[12] studied the effect of constitutive laws used to describe the thin membrane of the shell, on flow induced capsule deformation. The three laws used were Hooke's law Mooney-Rivlin and Skalak law and applied them on small and large deformations of the microbubble. They found that in the asymptotic limit of small deformations the three laws tend to produce similar results and reduce to the linear model of the shell, whereas when large deformations are applied, they produce dissimilar results with Mooney-Rivlin law describing strain-softening materials and Skalak law strain-hardening materials. Pelekasis and Tsiglifis, (2008) followed a similar approach for the modeling of the bubble shell. They used the Keller-Miksis[6] equation for the mathematical representation of the bubble motion and examined numerically how the viscoelastic behavior of the membrane along with the external liquid attributes such viscosity, compressibility and nonlinearity in the acoustic disturbance affect the response of the bubble. They found that the resonance frequency of strain softening material decreases with increasing amplitude, whereas the opposite occurs for strain hardening materials. They also investigated the effects of scattering on the bubble surface and concluded that the total scattering cross section of a Skalak membrane increases with increasing amplitude, while for Mooney-Rivlin and Kelvin-Voight membranes tends to decrease. Gong, Cabodi and Porter, (2014)[17] addressed the dependency of the viscoelastic properties of the shell to pressure suggesting a non-Newtonian behavior. They studied the pressure dependent resonance in lipid coated monodisperse microbubbles driven at low pressures utilizing a modified Rayleigh-Plesset equation. An experimental investigation was conducted, and the results were compared to theoretical predictions. They observed a noticeable shift in resonance frequency for free bubbles with a varying imposed disturbance while for coated microbubbles the resonance occurred at relatively stable values, indicating that the shift occurs due to primarily a change in the shell properties and not non-linear oscillations. To account for the shell structure, they employed a model for an effective surface tension proposed by Marmottant, (2005)[14] and modified it by varying the elastic modulus which was taken to be a function of pressure. They found that insonated coated microbubbles described by their model shifted towards the resonance frequency of a free microbubble with an accompanying reduction of the shell elasticity constant indicating a strain softening behavior of the shell. Naude, Mendez et al, (2020)[20] used a modified version of the Rayleigh-Plesset equation for a Mooney-Rivlin encapsulated bubble to describe its radial dynamics. They considered the thickness of the shell to be infinitesimally small and applied small acoustic disturbances in the far field. They used a perturbation approach for small values of the disturbance amplitude, whereas for bigger values a numerical solution was employed. In their asymptotic analysis they assumed that the amplitude of the external disturbance is of the third order and the bubble oscillates around its equilibrium radius with an amplitude of the first order. Viscous damping, namely the inverse of the Reynolds number of the liquid were of the second order. A multiple time scale analysis was executed and results for different parameters of the membrane elasticity and parameters regarding the flow , indicated that nonlinear resonance occurs in frequencies higher than the linear resonance frequency, a contradicting result when compared to the numerical results of Pelekasis and Tsiglifis[15].

In the present study the approach for the problem formulation is the one followed by Pelekasis and Tsiglifis[15]. The Keller-Miksis[6] model for the bubble dynamics is used along with the Kelvin-Voight (KV), Mooney-Rivlin (MR) and Skalak (SK) constitutive laws for each case of the membrane material. An asymptotic expansion scheme, the fundamentals of which are presented by Jordan and Smith[1] in their book for nonlinear ordinary differential equations, is used in an attempt to obtain approximate analytical solutions for an encapsulated microbubble immersed in a slightly compressible liquid subject to an oscillating ambient pressure field. Radial volume oscillations are studied and the results regarding the main resonance cases are depicted in amplitude-frequency figures and the results obtained are compared to those attained numerically by Pelekasis and Tsiglifis[15] for various sets of parameters.

The remainder of the present of the present study contains a presentation of the mathematical formulation of the problem in chapter 2, the asymptotic analysis application in chapter 3, a brief presentation of the numerical process followed by Pelekasis and Tsiglifis[15] in chapter 4, an application for the free bubble case and literature review in chapter 5 , a presentation of the results obtained analytically for free and encapsulated bubbles and a comparison with the numerical results of Pelekasis and Tsiglifis in chapter 6 and finally conclusions and suggestions for further studies in chapter 7.

2 Problem Formulation

2.1 Initial state of the problem

In the present study we examine the non-linear oscillations of bubbles encapsulated in an elastic shell. To do so we must first determine the state of the problem.

The initial conditions of the problem refer to the equilibrium state of a bubble submerged in a Newtonian fluid of density ρ_l and constant dynamic viscosity μ_l. The undisturbed static pressure of the surrounding liquid is taken to be uniform and equal to P'_{st}. We also account for compressibility phenomena in the surrounding liquid which may be small but not negligible. The initial microbubble of radius R_0 containing an insoluble ideal gas has a viscoelastic membrane surrounding it. It is considered volume incompressible with shear modulus G_s and viscosity μ_s. The shell thickness δ is taken to be much smaller than the initial radius R_0. Any effects of residual stresses are neglected so that at the equilibrium state the bubble is considered spherical and free of stresses. The gas pressure inside the bubble is considered uniform and constant at $P_{b,0}$

We investigate the bubble response to a disturbance imposed on the far pressure field. In this case the ambient pressure in the field is the sum of the static pressure and the imposed acoustic disturbance:

$$P'_\infty = P'_{st} + P'_{ac} \tag{2.1}$$

where P'_{ac} is the sinusoidal pressure disturbance:

$$P'_{ac} = \eta P'_{st} sin(\omega_f t')$$

where $\eta P'_{st}$ is the disturbance amplitude and ω_f is the angular forcing frequency lying in the ultrasound range. The above expression is a close approximation of the pressure distribution in the liquid for the case of an imposed disturbance whose wavelength is large compared to the radius of the affected bubble. (Prosperetti 1974)[3]

To specify the internal pressure of the bubble we assume that the liquid remains isothermal throughout the process. This uncouples the internal with external pressure and we can calculate the former without accounting for the external phenomena. The internal pressure is taken to be P_b and its variations are applied instantaneously and uniformly throughout the gas due to its negligible density and viscosity. In general, it is calculated through the application of conservation laws inside the bubble but for the present study a simpler approach is used where we assume adiabatic behavior for the bubble, thus the bubble volume-pressure relation reads

$$P'_{b,0} V'^{\gamma}_0 = P'_b V'^{\gamma} \tag{2.2}$$

where zero index denotes equilibrium state and γ is the adiabatic polytropic constant which remains constant throughout the motion. Assuming a stress-free state for the initial state on the interface, $P_{b,0}$ is related to the ambient pressure through the Young-Laplace equation

$$P_{b,0} = P_{st} + \frac{2\,\sigma}{R_0} \tag{2.3}$$

Equation 2.2 is applicable when thermal damping is neglected since such phenomena cause a phase difference between pressure and volume variations. This assumption is valid for smaller bubbles where the heat transfer time scale is fast compared to that of the problem under consideration. For bubbles of bigger radii thermal dissipation and acoustic attenuation should be taken under consideration. This can be achieved by introducing effective viscosities that account for thermal and acoustic damping and adding dissipative terms proportional to the velocity of the interface in the following equations. In this way valid approximate results can be deduced from the governing equations of the problem ,Prosperetti ,(1974)[3]

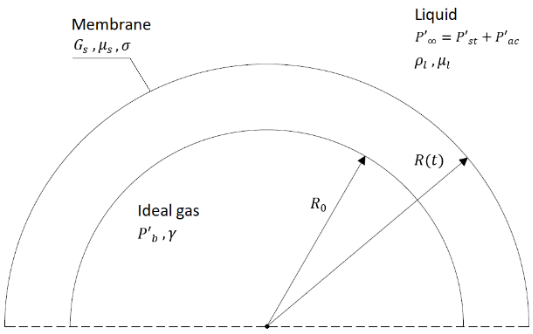

Fig 1 Bubble model in an infinitely extended, slightly compressible liquid with parameters and notation used.

2.2 Governing Equations

2.2.1 Flow formulation

As stated above we consider a microbubble, submerged in a Newtonian fluid, that undergoes time dependent change of volume containing an ideal gas. It remains spherical throughout the entirety of the motion and thus, its surface only moves in the radial direction. It follows that the liquid motion is strictly radial too. With the assumption of spherical symmetry, the motion of the liquid can be described by the radial component of equations of continuity and momentum. The viscous term in the momentum equation has been omitted since it enters through the liquid's compressibility which we assume to be small. Since a purely radial motion is also irrotational we introduce a velocity potential.

$$\boldsymbol{u} = \frac{\partial \boldsymbol{\varphi}}{\partial r}$$

$$\frac{\partial \rho}{\partial t} + \boldsymbol{\nabla} \cdot (\rho \mathbf{u}) = 0$$

$$\frac{\partial \boldsymbol{u}}{\partial t} + \boldsymbol{u}\frac{\partial \boldsymbol{u}}{\partial r} + \frac{1}{\rho}\frac{\partial p}{\partial r} = 0$$

To complete the formulation, we account for the kinematic condition at the membrane $r = R(t)$. For a purely radial motion with no net mass flux across the interface, since the bubble only contains insoluble gas, we obtain

$$u[r = R(t), t] = \frac{dR}{dt}$$

By assuming an incompressible model in the near vicinity of the bubble, the flow is described by the modified Bernoulli equation Keller Miksis, (1980)[6] or the Laplacian Prosperetti and Lezzi, (1986)[7], whereas the far field flow is described by a compressible formulation and thus the standard wave equation is appropriate. Far from the bubble refers to any distance that is comparable to the distance traveled by sound in the time scale of the problem, while near refers to distances close to the bubble equilibrium radius R_0.

Utilizing the above observations for the governing equations of the motion, we get a nonlinear second order ordinary differential equation for the bubble radius, describing spherosymmetric oscillations of a microbubble in a compressible fluid, it is the Keller-Miksis[6] model describing moderate, fast, or even very fast radial oscillations by properly accounting for compressibility effects Pelekasis and Tsiglifis, (2008) [15].

$$\left(1-\frac{\dot{R}'}{c'}\right)\ddot{R}'R'+\left(\frac{3}{2}-\frac{\dot{R}'}{2c'}\right){\dot{R}'}^2 = \left(1+\frac{\dot{R}'}{c'}\right)\frac{1}{\rho'}(P'_l-P'_\infty)+R'\frac{1}{\rho' c'}\frac{d}{dt'}(P'_l-P'_\infty) \qquad 2.4$$

When solved it provides the instantaneous location of the bubble's interface once the pressure field is known. To determine the liquid pressure in the interface we use a normal stress balance in the membrane. The normal component of the viscous stresses applied on the microbubble is given by

$$\boldsymbol{n}\cdot\boldsymbol{X}'_l\cdot\boldsymbol{n}|_{r'=R'}=\mu_l\left(2\frac{\partial u'_r}{\partial r'}-\frac{2}{3}\boldsymbol{\nabla}'\cdot\boldsymbol{u}'\right) \qquad 2.5$$

where the second term of the right-hand side is a result of compressibility and can be omitted for slightly compressible fluids without losing any validity of the Keller-Miksis[6] model. Prosperetti and Lezzi, (1986)[7]

When the shell thickness is infinitesimally small the external and internal radii coincides and thus, a single force balance can be written for the gas-liquid interface depending on the constitutive law describing the bubble membrane Pelekasis and Tsiglifis, (2008) [15].

$$[P'_B\boldsymbol{I}-P'_l\boldsymbol{I}+\boldsymbol{X}'_l]\cdot n=\sigma(\boldsymbol{\nabla}'_S\cdot\boldsymbol{n})\cdot\boldsymbol{n}-\boldsymbol{\nabla}'_S\cdot\boldsymbol{X}'_M \qquad 2.6$$

where n is the normal unit vector on the surface pointing outwards in the liquid, $\boldsymbol{I}$ the two-dimensional unit tensor, P_B' , P_l' the dimensional pressure inside the bubble and liquid pressure respectively, $\boldsymbol{X}_l', \boldsymbol{X}_M'$ the stress tensors of the liquid and membrane, σ then interfacial tension between the membrane and the surrounding liquid and $\boldsymbol{\nabla}_S'$ the surface gradient operator.

Equation 2.6 shows that the internal gas pressure P_B' exceeds the pressure of the liquid at $r = R(t)$ by surface tension effects, the normal component of the liquid's viscous stress and membrane viscous and elastic stresses. In the above equation liquid viscosity is being retained even though it is not included in the momentum equation.

2.2.2 Viscoelastic behavior of the shell

There are three constitutive laws describing the stresses that develop on the membrane, each one referring to the stress strain behavior of the material forming it. The analysis followed for the stress-strain behavior of the bubble membrane is in conformity with the one used by Pelekasis and Tsiglifis, (2008) [15].

Linear stress strain behavior

Kelvin-Voight model [KV] relates the viscoelastic stresses $\boldsymbol{X'}_M$ to the strain $\boldsymbol{\Gamma}'$ and rate of strain $\dot{\boldsymbol{\Gamma}}'$ tensors in a linear way. It's a generalized Hooke's law with the addition of a viscous term and therefore it is only applicable in the case of small membrane displacements. The above modeling reads

$$\boldsymbol{X'}_M = 2\left(G_s\boldsymbol{\Gamma}' + \mu_s\dot{\boldsymbol{\Gamma}}'\right)$$
$$\boldsymbol{\Gamma}' = \frac{1}{2}[\boldsymbol{\nabla}'\boldsymbol{u}' + (\boldsymbol{\nabla}'\boldsymbol{u}')^T] \quad \dot{\boldsymbol{\Gamma}}' = \frac{1}{2}[\boldsymbol{\nabla}'\boldsymbol{w}' + (\boldsymbol{\nabla}'\boldsymbol{w}')^T] \qquad 2.7$$

where u' , w' are the dimensional displacement and velocity of the membrane respectively, G_s the shear modulus and μ_s the membrane viscosity.

Non-linear stress-strain behavior

Most materials do not respond to external stresses in a linear way, they instead exhibit a varying slope in their stress strain relation at large deformations or at abrupt changes of pressure as it is in the case of ultrasound. Materials with non-linear behavior can be strain softening or strain hardening. The former case corresponds to an increasing shear stress modulus as the strain grows whereas the latter to a decreasing one. Taking these deviations from the linear model into consideration and using the appropriate expressions for the membrane stress tensor leads to more accurate results.

In the case of strain softening materials, a typical strain energy describing a very thin sheet of isotropic, volume incompressible material is the one provided by the two-dimensional Mooney-Rivlin model.

$$w^{MR} = \frac{G^{MR}}{2}\left[(1-b)\left(I_1 + 2 + \frac{1}{I_2+1}\right) + b\left(\frac{I_1+2}{I_2+1} + I_2 + 1\right)\right] \qquad 2.8$$

$$X'^{MR}_{M_{11}} = \frac{G^{MR}}{\lambda_1\lambda_2}\left(\lambda_1^2 - \frac{1}{(\lambda_1\lambda_2)^2}\right)[1 + b(\lambda_2^2 - 1)]$$

In the present study we set the constant b, which indicates the material softness, equal to zero. That is the case of a neo-Hookean membrane which represents the appropriate linear stress strain relationship that accounts for the change in metric properties during deformation Pelekasis and Tsiglifis, (2008) [15].

For the strain hardening case we use the constitutive law proposed by Skalak[2]

$$w^{SK} = \frac{G^{SK}}{2}(I_1^2 + 2I_1 - 2I_2 + CI_2^3) \qquad 2.9$$

$$X'^{SK}_{M_{11}} = \frac{G^{SK}}{\lambda_1\lambda_2}\lambda_1^2(\lambda_1^2 - 1) + C(\lambda_1\lambda_2)^2[(\lambda_1\lambda_2)^2 - 1]$$

Parameter C which represents the membrane area compressibility is always positive and for the present study we set $C = 1$

In the above expressions I_1 , I_2 denote the two-dimensional strain invariants and λ_1 , λ_2 the principal extension ratios. In the case of spherosymmetric oscillations the two principal extension ratios are equal

$$\lambda(t) = \lambda_1 = \lambda_2 = \frac{R'(t)}{R_0}$$

Substituting equations 2.7, 2.8, 2.9 into the normal stress balance 2.6 for the membrane we obtain the following expressions connecting the internal bubble pressure to the host liquid pressure on the interface.

$$\text{KV}\ \ P_l|_{r=R} = P_b(R) - \frac{2\sigma}{R} - 4\mu_l\frac{\dot{R}}{R} - 4\cdot 3\delta\mu_s\frac{\dot{R}}{R^2} - 2\frac{3\delta G_s}{R}\left[\left(\frac{R}{R_0}\right)^2 - 1\right]$$

$$MR\ \ P_l|_{r=R} = P_b(R) - \frac{2\sigma}{R} - 4\mu_l\frac{\dot{R}}{R} - 4\cdot 3\delta\mu_s\frac{\dot{R}}{R^2} - 2\frac{\delta G_s}{R}\left[1 - \left(\frac{R_0}{R}\right)^6\right]$$

$$SK\ \ P_l|_{r=R} = P_b(R) - \frac{2\sigma}{R} - 4\mu_l\frac{\dot{R}}{R} - 4\cdot 3\delta\mu_s\frac{\dot{R}}{R^2} - 2\frac{\delta G_s}{R}\left[\left(\frac{R}{R_0}\right)^6 - 1\right]$$

Upon replacing the above equations in equation 2.1 we obtain a non-linear ordinary differential equation with time being the only independent variable which we proceed to solve for the microbubble radius $R(t)$.

2.3 Non-dimensional formulation

We set the initial bubble radius R_0 and $\sqrt{P_{b,0}/\rho}$ as the characteristic scales for length and velocity respectively. It follows that the characteristic temporal scale of the problem is

$$\frac{R_0}{\sqrt{P_{b,0}/\rho}}$$

Primed letters denote dimensional variables. When scaled with the above characteristic quantities the non-dimensional variables introduced are

$$\tau = \frac{t'\sqrt{P_0/\rho}}{R_0} \qquad \omega = {\omega'}_f\sqrt{\frac{\rho\, R_0^2}{P_0}} \qquad R = \frac{R'}{R_0} \qquad P = \frac{P'}{P_{b,0}}$$

Time derivatives are also converted to non-dimensional form.

$$\frac{dR'}{dt'} = \sqrt{\frac{P_0}{\rho}}\frac{dR}{d\tau} \qquad \frac{d^2R'}{d{t'}^2} = \frac{P_0}{\rho R_0}\frac{d^2R}{d\tau^2}$$

Substitution in equation 2.1 yields

$$\begin{aligned}(1 - M\dot{R})\ddot{R}R + \left(\frac{3}{2} - \frac{M\dot{R}}{2}\right)\dot{R}^2 \\ = (1 + M\dot{R})(P_l - P_{st} - P_{ac}) + MR\frac{d}{dt}(P_l - P_{ac})\end{aligned} \qquad 2.2$$

where pressure terms are non-dimensional and scaled with $P_{b,0}$, the internal pressure corresponding to the equilibrium radius.

The non-dimensional liquid pressure on the bubble interface given by the Kelvin-Voight, Mooney-Rivlin and Skalak constitutive laws is

$$\text{KV} \quad P_l|_{r=R} = \left[\frac{1}{R^{3\gamma}} - \frac{2}{We}\frac{1}{R} - \frac{4}{Re}\frac{\dot{R}}{R} - \frac{4m}{Re}\frac{\dot{R}}{R^2} - 2\frac{3G}{R}(R^2-1)\right] \tag{2.3}$$

$$\text{MR} \quad P_l|_{r=R} = \left[\frac{1}{R^{3\gamma}} - \frac{2}{We}\frac{1}{R} - \frac{4}{Re}\frac{\dot{R}}{R} - \frac{4m}{Re}\frac{\dot{R}}{R^2} - 2\frac{G}{R}\left(1-\frac{1}{R^6}\right)\right] \tag{2.4}$$

$$\text{SK} \quad P_l|_{r=R} = \left[\frac{1}{R^{3\gamma}} - \frac{2}{We}\frac{1}{R} - \frac{4}{Re}\frac{\dot{R}}{R} - \frac{4m}{Re}\frac{\dot{R}}{R^2} - 2\frac{G}{R}(R^6-1)\right] \tag{2.5}$$

In conclusion we introduce the dimensionless numbers we encounter throughout the study

$Re_l = \frac{\rho R_0 \sqrt{P_{b,0}/\rho}}{\mu_l}$ is the Reynolds number of the host liquid comparing inertial to viscous forces

$We = \frac{R_0 P_{b,0}}{\sigma}$ is the Weber number comparing inertial forces to the membrane's surface tension

$m = \frac{3\,\mu_s \delta}{\mu_l R_0}$ is the relative fluid to membrane viscosity

$G = \frac{\delta\, G_s}{R_0 P_{b,0}}$ is the dimensionless shear modulus describing the material's response to shear stress

$M = \sqrt{\frac{P_{b,0}}{\rho}}\frac{1}{c}$ is the Mach number comparing the radial velocity of the bubble to the sound speed in the host liquid

3 PERTURBATION SOLUTIONS

3.1 Kelvin-Voight constitutive law application

3.1.1 Preliminary Considerations

We focus our attention on oscillations around the equilibrium radius R_0. When R_d is the deviation from the initial state we model the oscillating radius as

$$R'(t) = R_0[1 + R_d(t)]$$

In dimensionless terms the above equation reads

$$R(\tau) = 1 + R_d(\tau)$$

Substituting and carrying out the calculations while ignoring terms of fourth and higher order equation (2.2) yields

$$\begin{aligned}
\ddot{R}_d + R_d\left[3\gamma - \frac{2}{We} + 12G\right] \\
&= -\eta P_{st} sin(\omega\tau) + \eta P_{st} R_d sin(\omega\tau) - \omega\eta M P_{st} cos(\omega\tau) \\
&+ \left[\dot{R}_d\left[-3\gamma M + \frac{2}{We}M - 12GM - \frac{4}{Re}(1+m)\right] + \alpha_1 R_d^2 - \frac{3}{2}\dot{R}_d^2\right] \\
&+ \left[\dot{R}_d R_d\left[(3\gamma - 1)3\gamma M - 12GM + \frac{4}{Re}(2+3m)\right]\right. \\
&\left. - \frac{4}{Re}M\ddot{R}_d(1+m) - \alpha_2 R_d^3 + \frac{3}{2}\dot{R}_d^2 R_d\right]
\end{aligned} \quad 3.1$$

where dotted letters denote differentiation with respect to the dimensionless time τ and the following expressions have been used

$$\alpha_1 = \frac{9}{2}\gamma(\gamma + 1) - \frac{4}{We} + 18G$$

$$\alpha_2 = \frac{\gamma}{2}(9\gamma^2 + 18\gamma + 11) - \frac{6}{We} + 24G$$

We extract the dimensionless natural frequency from equation 3.1

$$\omega_0 = \sqrt{3\gamma - \frac{2}{We} + 12G} \qquad 3.2$$

which reverting to dimensional terms reads

$$\omega'_0 = \sqrt{\left(3\gamma P_0 - \frac{2\sigma}{R_0} + 12\frac{\delta G_s}{R_0}\right)\frac{1}{\rho R_0^2}}$$

We are concerned with the steady state of the motion and thus no initial conditions were defined. For this purpose, we set

$$R_d(\tau = 0) = 0 \quad \dot{R}_d(\tau = 0) = 0 \quad \ddot{R}_d(\tau = 0) = 0$$

3.1.2 Ordering

The dynamics of time dependent changes in a bubble radius that differs slightly from the initial equilibrium state can be studied analytically with regular asymptotic approximations. For this purpose, terms involved with nonlinearities are assumed to be small and need to be scaled with a reference parameter.

We proceed by assigning each term its respective order of magnitude, where the ε is the reference artificial parameter. The amplitude of the external disturbance is set to be of the second order. The resonant response of the bubble radius is of the first order. Since we are concerned with the response of the bubble near the main resonance, we also set the deviation of the forcing frequency from the linear resonance frequency, the detuning parameter, to be of the first order.

$$\begin{gathered} \eta P_{st} = \xi = \varepsilon^2 P \\ R_d = \varepsilon R_D \\ \left(\frac{\omega_0}{\omega}\right)^2 = 1 + \varepsilon\omega_1 \end{gathered} \tag{3.3}$$

where $P_{st} = {P'_{st}}/{P_{b,0}}$ is the dimensionless static pressure scaled with the internal bubble pressure at equilibrium. In the analysis presented herein P is set to 1 without any loss in generality as it represents the ordering between pressure disturbance and radial pulsations.

A weakly damped case is investigated. The total damping of the system is attributed to terms stemming from viscosity and compressibility phenomena. So, for damping to be small, both Mach and the inverse of Reynolds numbers need to be of the first order.

$$\begin{gathered} M = \varepsilon\,\mu \\ {1}/{Re} = \varepsilon\, r \end{gathered} \tag{3.4}$$

The $O(\varepsilon^2)$ forcing term in the ambient pressure leads to an $O(\varepsilon)$ change in the bubble radius. That is asymptotically small but one order of magnitude larger than the forcing inducing the bubble motion since we are in the main resonance area. Parameters $R_D,\ \mu,\ r,\ \omega_1$ must be of order 1 for the following asymptotic analysis to be valid. To simplify our calculations, we introduce the following change in the time scale of the problem

$$T = \omega\tau$$

Lastly, the value assignment of the scaling parameter ε, does not affect the final results. As it can be seen each parameter enters the ordinary differential equation through its scaled form and consequently the effects of ordering are balanced out. Only the initial value of the small parameters affects the results obtained.

3.1.3 Jordan-Smith method application[1]

With ordering set and applying the near resonance condition equation (3.1) reads

$$
\begin{aligned}
\ddot{R}_D + R_D = & -\frac{\varepsilon P}{\omega_0^2} sin(T) + \varepsilon^2 \left[-\frac{\mu P}{\omega_0} cos(T) - \frac{P}{\omega_0^2} \omega_1 sin(T) + \frac{P R_d}{\omega_0^2} sin(T) \right] \\
& + \varepsilon \left\{ -\dot{R}_D \left[\mu\omega_0 + \frac{4r(1+m)}{\omega_0} \right] + \frac{\alpha_1 R_D^2}{\omega_0^2} - \frac{3}{2} \dot{R}_D^2 - \omega_1 R_D \right] \\
& + \varepsilon^2 \left\{ -\dot{R}_D \left[\frac{\mu\omega_0\omega_1}{2} - \frac{2r\omega_1}{\omega_0} (1+m) \right] - 4r\mu \ddot{R}_D (1+m) \right. \\
& + \frac{\dot{R}_D R_D}{\omega_0} [(9\gamma^2 - 3\gamma)\mu - 12G\mu + 4r(2+3m)] - \frac{\alpha_2}{\omega_0^2} R_D^3 \\
& \left. + \frac{3}{2} \dot{R}_D^2 R_D + \frac{\alpha_1 R_D^2}{\omega_0^2} \omega_1 \right\} + O(\varepsilon^4)
\end{aligned}
\qquad 3.5
$$

where dotted variables represent differentiation with respect to the new time scale T. The solution of 3.5 is a function of both ε and T.

We assume this form to be a power series expansion of ε

$$
R_D(\varepsilon, T) = R_{D_0}(T) + \varepsilon R_{D_1}(T) + \varepsilon^2 R_{D_2}(T) + \cdots \qquad 3.6
$$

We now substitute the series (3.6) into equation (3.5). In order that the series solution satisfies the differential equation (3.5) with accuracy $O(\varepsilon^3)$, we balance out the coefficients of the same powers of ε, up to the second order. This results in a system of recursive second order linear differential equations each one of them yielding a solution for $R_{D_i}(T)$.

$$\boldsymbol{O(\varepsilon^0)} \quad \ddot{R}_{D_0} + R_{D_0} = 0 \tag{3.7}$$

$$\boldsymbol{O(\varepsilon^1)} \quad \ddot{R}_{D_1} + R_{D_1} = -\frac{P}{\omega_0^2} sin(T) - \dot{R}_{D_0}\left[\mu\omega_0 + \frac{4r}{\omega_0}(1+m)\right] + \frac{\alpha_1 R_{D_0}^2}{\omega_0^2} - \frac{3}{2}\dot{R}_{D_0}^2 - \omega_1 R_{D_0} \tag{3.8}$$

$$\begin{aligned}\boldsymbol{O(\varepsilon^2)} \quad \ddot{R}_{D_2} + R_{D_2} = & -\frac{P}{\omega_0^2}\omega_1 sin(T) - \frac{\mu P}{\omega_0} cos(T) + \frac{P}{\omega_0^2} R_{D_0} sin(T) \\ & - \dot{R}_{D_0}\left[\frac{\mu\omega_0\omega_1}{2} - \frac{2r\omega_1}{\omega_0}(1+m)\right] \\ & - \dot{R}_{D_1}\left[\mu\omega_0 - \frac{4r}{\omega_0}(1+\ m)\right] - 4r\mu\ddot{R}_{D_0}(1+m) \\ & + \frac{R_{D_0}\dot{R}_{D_0}}{\omega_0}[(9\gamma^2 - 3\gamma)\mu - 12G\mu + 4r(2+3m)] \\ & - \frac{\alpha_2}{\omega_0^2} R_{D_0}^3 + \frac{\alpha_1\omega_1}{\omega_0^2} R_{D_0}^2 + \frac{2\alpha_1}{\omega_0^2} R_{D_0} R_{D_1} \\ & + \frac{3}{2}\dot{R}_{D_0}^2 R_{D_0} - 3\dot{R}_{D_1}\dot{R}_{D_0} - \omega_1 R_{D_1}\end{aligned} \tag{3.9}$$

We are searching for periodic solutions having the period, 2π, of the forcing term. This condition reads

$$R_{D_i}(T + 2\pi) = R_{D_i}(T)\,, \quad i = 0,1,2, \ldots$$

The $O(\varepsilon^0)$ equation represents the linearized equation. When $\varepsilon = 0$, all nonlinear terms vanish, and a resonant, simple harmonic, motion with zero damping is obtained. According to the assumption made for the solutions of (3.5), the power series expansion (3.6) shows that the solution to the nonlinear equation deviates from the zeroth order solution for the linearized case. This indicates that the features of the linear motion will be, to some extent, preserved to the weakly non-linear case examined for small values of the parameter ε.

For the resonant case the forcing terms coincide with the solution of the homogeneous equation. When such forcing terms are present, a particular solution cannot exist in the form $Csin(T)$. This leads to terms that are of the form $CTsin(T)$ which for $T \ll 1$ might not exhibit abnormal behavior but as T approaches infinity at steady state, they become unbounded, and therefore do not satisfy condition (3.7). Such terms, known as secular, should consequently be balanced out by the other terms present in the above equations for the assumed asymptotic expansion to provide valid approximations for all T.

Taking the above into consideration we choose an appropriate solution for each equation in such a manner that it negates any secular terms present in the next order of approximation equation. This defines the solution of the linearized equation (3.7) as the one eliminating secular terms in the first order equation (3.8). The same process is followed for the next orders of equations.

The general solution of (3.4) with A_0, B_0 arbitrary constants is

$$R_{D_0} = A_0 cos(T) + B_0 sin(T) \qquad 3.10$$

We substitute equation 3.10 into equation 3.8 and then identify the coefficients of secular terms by integration. Multiplying the right-hand side of equation 3.8 with $sinT$ and then integrating with respect to T, from 0 to 2π, yields an expression for the $sinT$ coefficients. The terms that survive the integration are the coefficients of $sinT$ since the product of its integration is π and any other trigonometric function of T is eliminated when multiplied by $sinT$ and then integrated with respect to T, from 0 to 2π. In the same manner we derive an expression for the $cosT$ coefficients by multiplying the right-hand side of equation 3.8 with $cosT$ and carrying out the same integration. Equating both resulting expressions to zero provides a system of two algebraic equations with the two unknowns being the constants A_0, B_0.

$$-\frac{B_0\mu\omega_0^2 + A_0\omega_0\omega_1 + 4B_0 r(1+m)}{\omega_0} = 0$$

$$\frac{A_0\mu\omega_0^3 - B_0\omega_0^2\omega_1 - P + 4A_0\omega_0 r(1+m)}{\omega_0} = 0$$

Solving the above system of equations yields

$$A_0 = \frac{{}^{P}\!/_{\omega_0}\,[\mu\omega_0^2 + 4r(1+m)]}{[\mu\omega_0^2 + 4r(1+m)]^2 + (\omega_0\omega_1)^2}$$

$$B_0 = -\frac{\omega_1 P}{[\mu\omega_0^2 + 4r(1+m)]^2 + (\omega_0\omega_1)^2}$$

where $\mu\omega_0 + \frac{4r(1+m)}{\omega_0}$ is the total damping of the problem due to viscous forces and compressibility effects. In this way we define the R_{D_0} solution of the $O(\varepsilon^0)$ equation by eliminating any secularity present in the $O(\varepsilon^1)$ equation. We proceed by finding the general solution of equation (3.5) which now does not contain any secular terms. That is

$$R_{D_1} = A_1 cos(T) + B_1 sin(T) + \left(\frac{\alpha_1}{\omega_0^2} - \frac{3}{2}\right)\frac{A_0^2 + B_0^2}{2} - \left(\frac{\alpha_1}{3\omega_0^2} + \frac{1}{2}\right)\frac{A_0^2 - B_0^2}{2}$$
$$- \left(\frac{\alpha_1}{3\omega_0^2} + \frac{1}{2}\right) A_0 B_0 sin(2T)$$

Substituting in (3.9) and carrying out the same integration procedure that was used for the $O(\varepsilon^1)$ equation, we define the A_1, B_1 coefficients, by eliminating secular terms in the $O(\varepsilon^2)$ equation.

The resultant system of equations deriving from the integrations of the right-hand side of equation 3.9 which we will solve for A_1, B_1 is

$$A_1[\mu\omega_0^2 + 4(1+m)] - B_1\omega_0\omega_1 = D_1$$

$$A_1\omega_0\omega_1 + B_1[\mu\omega_0^2 + 4(1+m)] = D_2$$

where

$$D_1 = -\mu P + 4\omega_0 \mu r(1+m)A_0 - \frac{[\mu\omega_0^2 + 4r(1+m)]B_0\omega_1}{2} + \frac{A_0 C(A_0^2 + B_0^2)}{24\omega_0^3}$$

$$D_2 = \frac{\omega_1}{\omega_0}P - 4\omega_0 \mu r(1+m)B_0 - \frac{[\mu\omega_0^2 + 4r(1+m)]A_0\omega_1}{2} - \frac{B_0 C(A_0^2 + B_0^2)}{24\omega_0^3}$$

$$C = 20\alpha_1^2 - 30\alpha_1\omega_0^2 + 18\alpha_2\omega_0^2 + 27\omega_0^4$$

The resulting expressions for the first order approximation of the amplitude A_1, B_1 are

$$A_1 = \frac{[\mu\omega_0^2 + 4r(1+m)]D_2 + D_1\omega_0\omega_1}{[\mu\omega_0^2 + 4r(1+m)]^2 + (\omega_0\omega_1)^2}$$

$$B_1 = \frac{[\mu\omega_0^2 + 4r(1+m)]D_1 + D_2\omega_0\omega_1}{[\mu\omega_0^2 + 4r(1+m)]^2 + (\omega_0\omega_1)^2}$$

With coefficients identified, the deviation of the bubble radius from the equilibrium state is given by

$$\begin{aligned} R_d = \frac{R(t) - R_0}{R_0} = \varepsilon R_D \\ &= (A_0 + \varepsilon A_1 + \ldots)cos(T) + (B_0 + \varepsilon B_1 + \ldots)sin(T) + O(\varepsilon^2)sin(2T) \\ &+ O(\varepsilon^2)cos(2T) \end{aligned}$$

Consequently, the amplitude of the fundamental oscillation, which is a function of the main resonance deviation ω_1 from the linear resonance frequency, reads as

$$\frac{R_{max} - R_0}{R_0} = R_{d,max} = \varepsilon R_{D,max} = \varepsilon\sqrt{(A_0 + \varepsilon A_1)^2 + (B_0 + \varepsilon B_1)^2} \qquad 3.11$$

It is the above expression that we shall use in the upcoming paragraphs to obtain the resonance curve and pinpoint the frequency in which we get the maximum response and its value for a given set of parameters describing the excitation and the physical properties of the system.

3.2 Mooney-Rivlin and Skalak constitutive laws

The same procedure is followed for the remaining two constitutive models for the microbubble membrane. Carrying out the calculations for each model results in similar equations for each order of ε. The terms that differ for each model *and* are not involved in α_1 and α_2 expressions, do not contribute to identifying the amplitude coefficients since they do not exhibit secular behavior. It follows that the equations yield the same form for the amplitude of radius deviation from the initial state, with the difference being with the α_1, α_2 parameters and more specifically the terms that stem from the dimensionless shear stress modulus.

<u>Mooney Rivlin</u>

$$\alpha_1 = \frac{9}{2}\gamma(\gamma + 1) - \frac{4}{We} + 66G$$

$$\alpha_2 = \frac{\gamma}{2}(9\gamma^2 + 18\gamma + 11) - \frac{6}{We} - 232G$$

<u>Skalak</u>

$$\alpha_1 = \frac{9}{2}\gamma(\gamma + 1) - \frac{4}{We} - 6G$$

$$\alpha_2 = \frac{\gamma}{2}(9\gamma^2 + 18\gamma + 11) - \frac{6}{We} + 16G$$

Regarding the natural frequency of the bubble, since it was assumed in the previous sections that the parameters referring to the membrane compressibility and softness are respectively $C = 1$, $b = 0$, it is deduced that when

$$\mu_{MR} = 3\delta'\mu_s \text{ and } G_{MR} = \delta' G_s$$

$$\mu_{SK} = 3\delta'\mu_s \text{ and } G_{SK} = \delta' G_s$$

for the MR and SK constitutive laws, the same is expression is recovered as in the KV case, equation 3.2. We conclude that the microbubble linear resonant frequency is independent of the membrane constitutive law. The nonlinear resonance and nonlinear behavior, however, differ for each case, when all terms of the problem are accounted for.

4 NUMERICAL IMPLEMENTATION

In the following segment a brief presentation of the numerical implementation will be given as it was conducted by Pelekasis and Tsiglifis[15]. In their study the resonance frequency as well as the scattering cross section of the fundamental and higher harmonics were monitored when moderate or large acoustic disturbances were applied, for each constitutive model for the bubble membrane.

The spherosymmetric oscillations of the bubble as they are described by the ordinary differential equation 2.2 paired with one of the three constitutive laws describing each case of the membrane's behavior is solved numerically via the explicit fourth order Runge-Kutta method which was chosen due to the increased numerical stability it provides and its $O(\Delta t^4)$ accuracy. To apply the method the second order nonlinear differential equations were converted to systems of first order differential equations. The time step of the numerical integration was maintained constant throughout the process and its value was selected so that enough steps could fit into one period of the induced oscillation, Pelekasis et al. (2004)[13]. The dimensionless period of the steady state forced oscillation is given by $T' = {}^{2\,\pi}/_{\omega_f}$ and its nondimensional counterpart is
$T = 2\pi$ when scaled with the driving frequency which defined the characteristic temporal scale in their analysis. It follows that a time step $\Delta\tau = 0.001$ is sufficiently small for enough iterations of the Runge-Kutta method in one period[11].

The dimensionless scattering cross section was calculated numerically through the resultant values of the numerical integration of equation 2.2 and equation 4.1

$$\sigma'_{Sc,n} = 4\pi \frac{\int_0^{t_f} \left(r' P'_{Sc,n}\right)^2 dt}{\int_0^{t_f} P'^2_{ac} dt} \qquad 4.1$$

and theoretically, when the linear solution of equation 2.2 was considered, as a function of the forcing frequency for small amplitudes and a standard set of parameter values.

$$\frac{\sigma'_{Sc}}{4\pi R_0^2} = \frac{1}{\left[\left(\frac{F_3}{F_1}\right)^2 - 1\right]^2 + \delta_t^2} \sqrt{\frac{1+M^2}{F_1^2}}\ , \delta_t = \frac{F_2}{F_1}$$

To compute the numerator integral of equation 4.1 Parseval's identity was employed.

$$\int_0^{t_f} f(t)^2 dt = \frac{t_f}{2} \sum_{n=1}^{\infty} (a_n^2 + b_n^2)$$

where t_f is the time integration duration and a_n, b_n are the Fourier coefficients of $f(t)$ which are calculated through the Fast Fourier Transform algorithm (FFT). When applied on the Fourier coefficients of the scattered pressure the zeroth order coefficients were omitted since they refer to the time average of the scattered pressure which does not contain neither the static pressure nor the acoustic disturbance and is approximately zero over the time integration.

The validity of the numerical implementation was investigated in the case of small pressure disturbances where the numerical results were compared against the predictions of the linear theory. Results were tested for convergence with respect to time step and agreement between the two methods had been established. Furthermore, as it was previously stated in the asymptotic solution employed in the above paragraphs, when ε<<1 and C=1 the tree constitutive laws predict the same dynamic behavior for the microbubble. However, when non-linear perturbations are applied the resulting dynamic behavior for each case is quite different.

5 FREE GAS BUBBLE OSCILLATIONS IN AN INCOMPRESSIBLE LIQUID

5.1 Asymptotic method implementation

We proceed by testing the validity of the asymptotic expansion scheme used in the present study by applying it to cases previously studied and compared the convergence of the results. For this purpose, the case that will be used is the one referring to a free microbubble immersed into an incompressible fluid subject to an acoustic sinusoidal disturbance imposed on the far field, as it was studied by Prosperetti[3] analytically, using a time-centered Krylov-Bogolyubov technique, Samek[5] with a slightly different approach on the analytical solution using the Bogolyubov-Mitropolskiy method and Lauterborn[4] numerically. The resulting behavior of the bubble motion as it is described by the asymptotic analysis attempted in the present study will be compared to the results obtained by the above authors.

To this end we adjust the governing equations, kinematic and dynamic boundary conditions to describe the problem of the free bubble as it was stated above. We begin by neglecting any compressibility effects. For this purpose, the Mach number of the flow is set to zero. In addition, any viscous or elastic effects of the microbubble shell must be neglected. This is achieved by setting the dimensionless shear stress modulus G comparing elastic with inertia forces equal to zero. Implementing these changes to the Keller-Miksis[6] model and to the normal stress balance, leads to the Rayleigh-Plesset equation describing the spherically symmetric oscillations of a bubble surrounded by an incompressible liquid which reads in dimensional form

$$R'\ddot{R}' + \frac{3}{2}\dot{R}'^2 = \frac{1}{\rho_l}\left[P'_b(R) - \frac{2\sigma}{R'} - \frac{4\mu_l}{R'}\dot{R}' - P'_\infty\right]$$

where R is the instantaneous bubble radius P'_b is the internal pressure of the bubble and P'_∞ is the ambient pressure of the external liquid.

The acoustic disturbance imposed on the far field is sinusoidal and as a result the ambient pressure oscillates with angular frequency ω_f about its average value P_{st}, with an amplitude η

$$P_\infty(t) = P'_{st}\left[1 - \eta cos\left(\omega_f\ t\right)\right]$$

The adiabatic assumption for the bubble behavior is retained, thus the internal pressure of the bubble can be calculated via the pressure volume equation introduced in equation 2.2. The introduction of effective viscosities can also be applied in the case of the free bubbles, for the case where thermal and acoustic damping cannot be neglected, as it was shown by Prosperetti[3] . The internal pressure of the bubble in the equilibrium state is also calculated by equation 2.3.

The same non-dimensional formulation is followed as it was showed in paragraph 2.3. Accounting for the incompressible fluid and the free surface of the bubble we eliminate the Mach number and the shear stress modulus respectively. The Rayleigh-Plesset equation reads in dimensionless terms

$$\ddot{R}R + \frac{3}{2}\dot{R}^2 = P_b - \frac{2}{We}\frac{1}{R} - \frac{4}{Re}\frac{\dot{R}}{R} - P_\infty$$

where the dimensionless numbers We, Re denoting the effects of surface tension and viscous damping respectively are defined in the same manner as in the case of the encapsulated bubble.

Following the same asymptotic expansion scheme for the free bubble, we seek the steady state solution for the bubble radius for the near main resonance case. Applying small perturbations in the bubble radius around its equilibrium radius and carrying out the calculations while ignoring terms of fourth and higher order leads to an equation identical to that obtained by Prosperetti[3].

Adjusting to the present study terminology it reads

$$\ddot{R}_d + \omega_0^2 R_d = \xi cos(\omega\tau) - \xi R_d cos(\omega\tau) + \xi R_d^2 cos(\omega\tau) + \left[-\frac{3}{2}R_d^2 - \frac{4}{Re}\dot{R}_d + \alpha_1 R_d^2\right] + \left[\frac{3}{2}R_d \dot{R}_d^2 - \alpha_2 R_d^3 + \frac{8}{Re}R_d \dot{R}_d\right] + O(\varepsilon^4) \quad 5.1$$

where

$$\alpha_1 = \frac{9}{2}\gamma(\gamma+1) - \frac{4}{We}$$

$$\alpha_2 = \frac{\gamma}{2}(9\gamma^2 + 18\gamma + 11) - \frac{6}{We}$$

$$\xi = \eta P_{st} = \left(1 - \frac{2}{We}\right)\eta$$

and ω_0 is the linear resonance frequency of the bubble in dimensionless terms

$$\omega_0 = \sqrt{3\gamma - \frac{2}{We}} \quad 5.2$$

We proceed by applying the near resonance condition equation 3.4 and expanding the deviation from the equilibrium radius R_d in a power series expansion of ε, equation 3.6. Using the same ordering for each of the parameter magnitudes as in paragraph 3.1.2 and substituting in equation 5.1 we obtain once again a recursive system of second order linear differential equations each one of them yielding a solution for $R_{D_i}(T)$.

$$\boldsymbol{O(\varepsilon^0)} : \ddot{R}_{D_0} + R_{D_0} = 0$$

$$\boldsymbol{O(\varepsilon^1)} : \ddot{R}_{D_1} + R_{D_1} = \frac{P}{\omega_0^2} cos(T) - \frac{4r}{\omega_0}\dot{R}_{D_0} + \frac{\alpha_1 R_{D_0}^2}{\omega_0^2} - \frac{3}{2}\dot{R}_{D_0}^2 - \omega_1 R_{D_0}$$

$$\begin{aligned}\boldsymbol{O(\varepsilon^2)} : \ddot{R}_{D_2} + R_{D_2} \\ &= \frac{P}{\omega_0^2}\omega_1 cos(T) - \frac{P}{\omega_0^2} R_{D_0} cos(T) - \left(\frac{2r\omega_1}{\omega_0} + \frac{4r}{\omega_0}\right)\dot{R}_{D_1} + \frac{8r}{\omega_0} R_{D_0}\dot{R}_{D_0} \\ &+ \frac{3}{2}\dot{R}_{D_0}^2 R_{D_0} - 3\dot{R}_{D_1}\dot{R}_{D_0} + \frac{\alpha_1\omega_1}{\omega_0^2} R_{D_0}^2 + \frac{2\alpha_1}{\omega_0^2} R_{D_0} R_{D_1} - \frac{\alpha_2}{\omega_0^2} R_{D_0}^3 - \omega_1 R_{D_1}\end{aligned}$$

Eliminating the secular terms present in the right-hand side of the ODEs in the same manner as before, paragraph 3.1.3, allows us to determine the A_i, B_i coefficients for each equation. Carrying out the same procedure yields

$$A_0 = \frac{\omega_1 P}{(\omega_1\omega_0)^2 + 4r^2} \qquad B_0 = \frac{\frac{P}{\omega_0} 2r}{(\omega_1\omega_0)^2 + 4r^2}$$

$$A_1 = \frac{\omega_1\omega_0 D_1 + 2BD_2}{(\omega_1\omega_0)^2 + 4r^2} \qquad B_1 = \frac{2BD_1 - \omega_1\omega_0 D_2}{(\omega_1\omega_0)^2 + 4r^2}$$

where,

$$D_1 = \frac{r_0^3 cos(\varphi_0) C}{24\omega_0^3} + \frac{P\omega_1 + r\omega_1\omega_0 r_0 sin(\varphi_0)}{\omega_0}$$

$$D_2 = \frac{r_0^3 sin(\varphi_0) C}{24\omega_0^3} - \mathrm{r}\omega_1\omega_0 \cos(\varphi_0)$$

$$C = 20\alpha_1^2 - 30\alpha_1\omega_0^2 - 18\alpha_2\omega_0^2 + 27\omega_0^4$$

The amplitude of the deviation of the bubble radius from the equilibrium state is given by

$$\frac{R_{max}-R_0}{R_0}=R_{d,max}=\varepsilon R_{D,max}=\varepsilon\sqrt{(A_0+\varepsilon A_1)^2+(B_0+\varepsilon B_1)^2}$$

This expression is the one we shall use to determine the maximum value of the amplitude of the bubble wall occurring for the near main resonance case, as well as the values of the frequency in which it appears.

5.2 Results and literature review

We procced by assigning values to the parameters, namely those used by Prosperetti,(1974)[3], to cross check results. The calculations are applied to systems of moderate damping, in which the bubble equilibrium radius is taken to be $R_0 = 10^{-6}m$, immersed in water at 20ºC. This implies the following properties for water $\rho = 998\, {}^{kg}/_{m^3}$, $\sigma = 0.0725\, {}^{N}/_{m}$, $\mu = 0.001\, {}^{kg}/_{ms}$. Furthermore, the undisturbed liquid static pressure is taken to be at $P_{st} = 1$bar. It follows that the dimensionless quantities ${}^{2}/_{We}$, ${}^{2}/_{Re}$ are taking the following values 0.592 , 0.128 respectively. Lastly, by letting the amplitude of the disturbance to be $\eta = 0.5$ the "effective pressure amplitude" ξ value is set to be 0.204.

With parameters set, carrying out the calculations leads to the expression yielding the amplitude of the deviation from the initial radius which will be plotted versus the normalized frequency to match the graphs it will be compared to

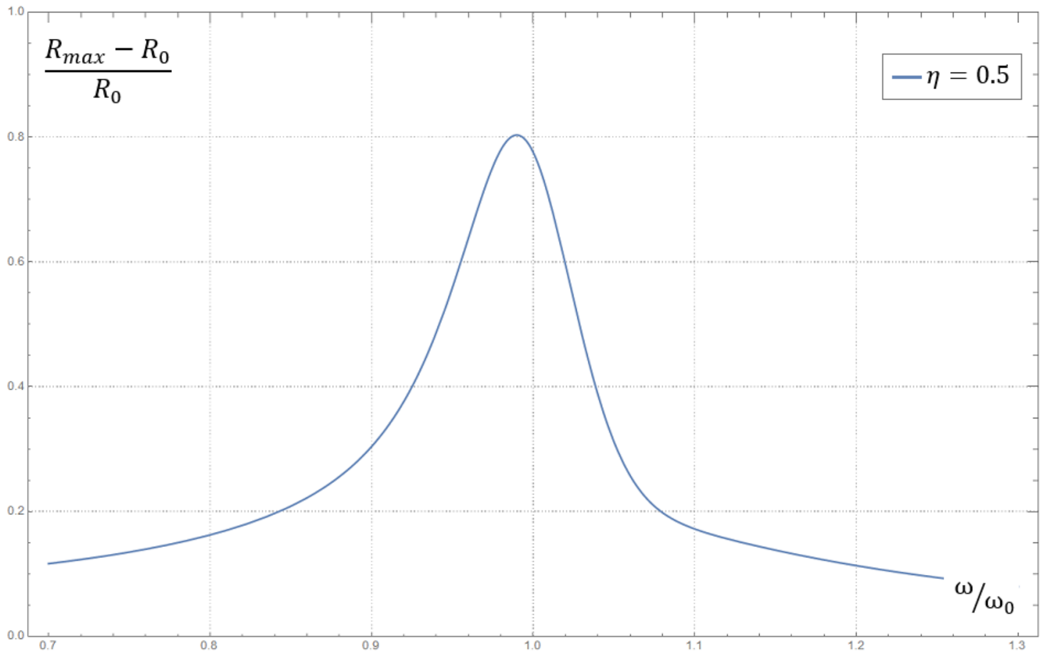

Fig5.1 *Amplitude of the deviation from initial radius for a free bubble $R_0 = 1\mu m$ in an incompressible liquid.*

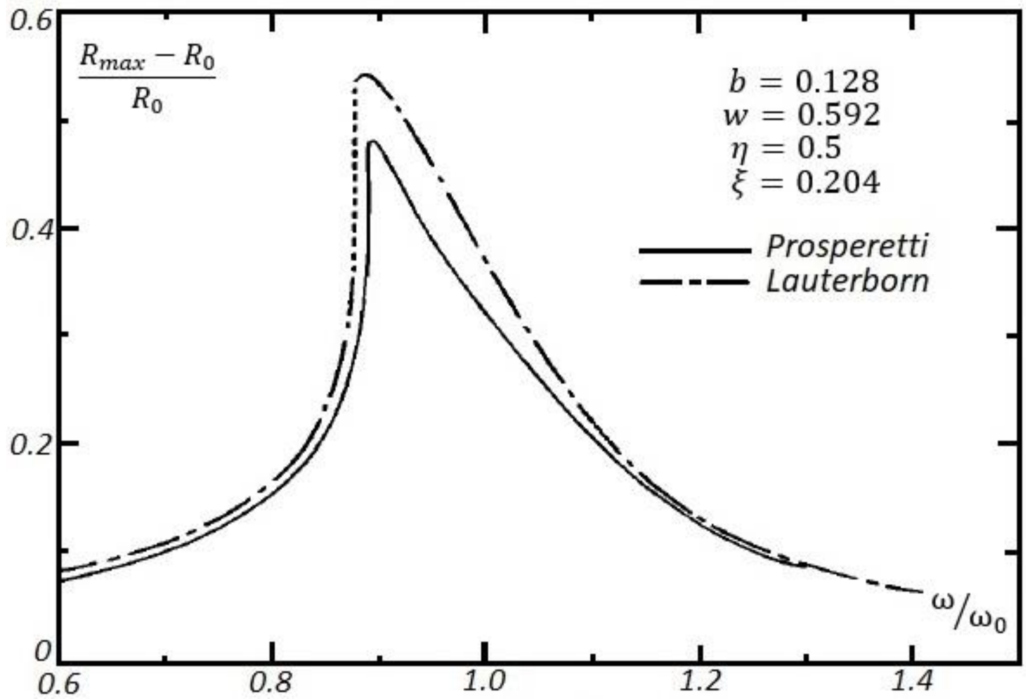

Fig5.2 *Amplitude of the deviation from initial radius for a free bubble $R_0 = 1\mu m$ in an incompressible liquid and as it was obtained analytically (Prosperetti[3]) and numerically (Lauterborn[4])*

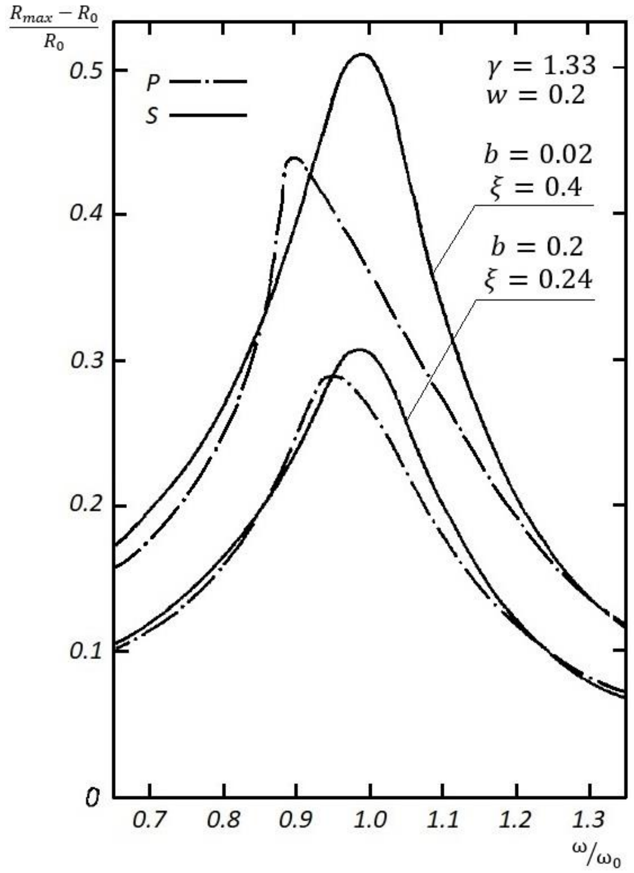

Fig5.3 *Amplitude of the deviation from initial radius for a free bubble $R_0 = 1\mu m$ in an incompressible liquid, compared results with Prosperetti (Samek[5])*

It can be seen from figures 5.1, 5.2, 5.3 that the maximum value of the nonlinear main resonance response is attained for frequencies lower than the natural frequency of the bubble. That frequency shift indicates a “soft spring” behavior ,on the average, for the system. A bubble behaves much like a soft spring system because on the average the softening on elongation overrides the hardening on compression Lauterborn, (1974)[4]. Jumping phenomena, meaning discontinuities in the response of the bubble, occur in the numerically attained figures depending on the direction of the frequency alteration.

Figure (5.2) depicting Lauterborn’s results shows two different stable branches for the response. As it was observed in his study, the lower one is reached by following the bubble’s response to a gradually increasing frequency from lower values to the near resonance area while the upper stable branch is reached by attaining a steady state solution for a higher frequency and reducing the frequency with small steps so that the maximum response is obtained without collapsing to the lower stable branch. A hysteresis behavior of the bubble’s response, regarding the stable branch followed, is evident from the above statement. On the same graph the expression obtained by Prosperetti[3] for the amplitude of the deviation from the initial radius is plotted. There is a good agreement between the two studies for the amplitude and frequency values and they were both able to capture the foldover in the resonance curve pointing in the direction of decreasing frequency values.

Samek[5] employed the Bogolyubov-Mitropolskiy method to extract the analytical solution to the Rayleigh-Plesset equation. His method yielded similar results to those of Prosperetti[3] with some overestimation regarding the magnitude of the amplitude. It also did not produce any foldover effects for the resonance curve, a defining property for nonlinear resonance phenomena.

The asymptotic scheme employed in the present study produced the results of figure 5.1. An overestimation of the resulting amplitude is evident compared to the values obtained by Prosperetti[3], Lauterborn[4] and Samek[5]. It was also not able to capture the foldover effect in the amplitude curve. This divergence in the amplitude values possibly stems from the ordering applied for the amplitude of the external disturbance and the values of the small parameter ε it produces. Both authors in their respective analytical studies assumed an amplitude of the first order $\xi \sim O(\varepsilon)$. The amplitude of the deviation from the initial radius of the steady state oscillation to the first approximation is given by

$$r_d = \frac{R_{max} - R_0}{R_0} = \frac{\xi}{\sqrt{4b^2\omega^2 + (\omega_0^2 - \omega^2)^2}}$$

Since the deviation is set to be of the first order $O(\varepsilon)$, the same must be applied to its amplitude. However, when the amplitude of the disturbance is scaled the way Prosperetti[3] proposed, it is deduced from the above expression that, for the main resonance case, where the forcing frequency deviates from the natural frequency by a term of the first order, equation 3.2, the resultant amplitude must be of order one $O(1)$, a counterintuitive result going against the initial assumption for the ordering of the deviation from the equilibrium radius. However, when the scaling for the amplitude of the external disturbance is done the way proposed by the present study and $\xi \sim O(\varepsilon^2)$, then the amplitude resulting from the above expression is in agreement with the initial assumption for the deviation.

It should be noted that the focus of the aforementioned studies expands beyond the main resonance to subharmonic and harmonic resonance cases. In the present study, however, we restrict our attention to the main resonance , although it should be evident from the analysis in paragraph 3.1.2 that it can be applied to subharmonic and harmonic resonance cases with some alterations regarding the expression used to describe the near resonance restriction.

Furthermore, upon reducing the amplitude of the pressure disturbance down to $\eta = 0.2$ or $\eta = 0.3$ and repeating the present analysis and calculation both the resonance frequency and maximal radial deviation $(R_{max} - R_0)/R_0$ are recovered with significant agreement to the numerical results of Pelekasis and Tsiglifis[15], as it will be seen in chapter 6 where a detailed comparison is presented between analytical and numerical solutions. Figures 6.2 and 6.8.

It is concluded that the asymptotic analysis employed in the present study produces valid results, considering the assumption made for the order of the disturbance holds true. In the next chapters it will be applied to encapsulated bubbles surrounded by a viscoelastic membrane to investigate the main resonance and how it is affected by the presence of the shell.

6 RESULTS AND DISCUSSION

In the present section a parametric study is conducted, investigating the effect of the microbubble properties and ultrasound characteristics on the response of the interface to the imposed disturbance. The amplitude as well as the resonance frequency of the fundamental harmonic are monitored when the acoustic disturbance is applied for each constitutive law governing the elastic behavior of the shell. The parameters used on this section are based on the available literature and are the same with those used by Pelekasis and Tsiglifis, (2008) [15] in their numerical study, to which the present results will be compared to. The responses presented in the following graphs refer to the steady state of the pulsation after transient motion of the bubble has elapsed.

6.1 Properties of the system

We restrict our investigations to encapsulated microbubbles immersed in water. The surrounding water temperature is set at 20° which determines its properties. The set of parameters describing the water density, dynamic viscosity and sound speed are respectively

$$\rho_l = 998 \,{}^{kg}\!/_{m^3} \;, \mu_l = 0.001 \,{}^{kg}\!/_{ms} \;, c_l = 1500 \,{}^{m}\!/_{s}$$

In the absence of any reliable data on membrane porosity, the interfacial tension is set to the average of the gas membrane and liquid-membrane tensions. It is almost the same as the gas-host fluid interfacial tension for the case of a shell with very small thickness. $\sigma = 0.072 \,{}^{kg}\!/_{s^2}$

Based on the experimental data Pelekasis and Tsiglifis[15] studied bubbles of radius $R_0 = 3\mu m$ with a characteristic shell thickness $\delta \approx 15nm$. The shear stress modulus G_s was limited to values between 35 and 105 MPa and the membrane dynamic viscosity μ_s to values ranging from 0.6 to 1.6 kg/ms. As it was stated before parameters b and C were set to 0 and 1 for the MR and SK constitutive laws respectively.

6.2 Compressibility effects on the free bubble case

In the present section the host liquid is taken to be slightly compressible. Although the compressibility phenomena are taken to be small, $M \to O(\varepsilon)$, the effects on the bubble's response are observed and worth noted. We begin by observing the case of a free gas bubble of initial radius $R_0 = 1\mu m$. As it can be seen in figures 6.1 and 6.2 when the liquid is compressible the maximum response $R_{d,max}$ is reduced significantly especially when then amplitude of the disturbance η is increased. An increasing Mach number acts as an additional damping factor, thus, leading to diminishing values of the bubble's amplitude. The natural frequency is still given by equation 5.2 for the free bubble since any compressibility phenomena do not affect the linear part of the problem from which the natural frequency stems from. The soft spring behavior of the system is retained in the compressible case, as it can be seen from the graphs, and the resonance occurs in lower than the natural frequencies due to the nonlinearities of the governing equations.

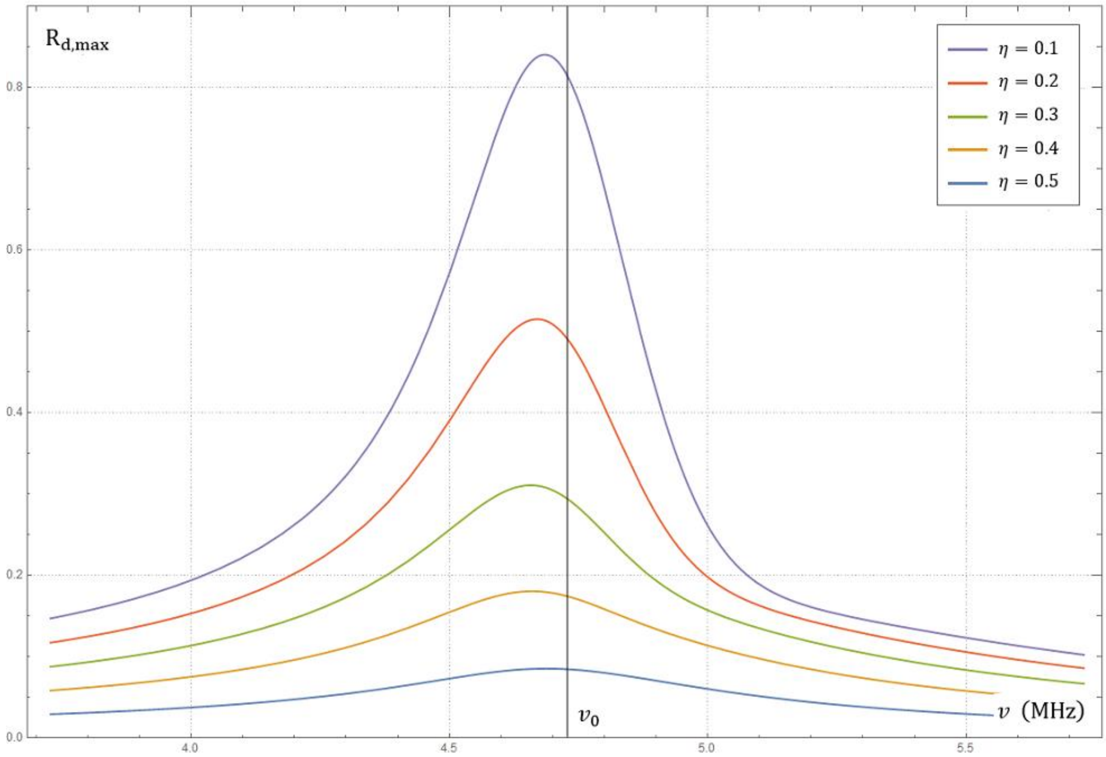

Fig.6.1 Response of a free bubble of initial radius R_0=1μm insonated by an external sinusoidal disturbance, immersed in incompressible liquid

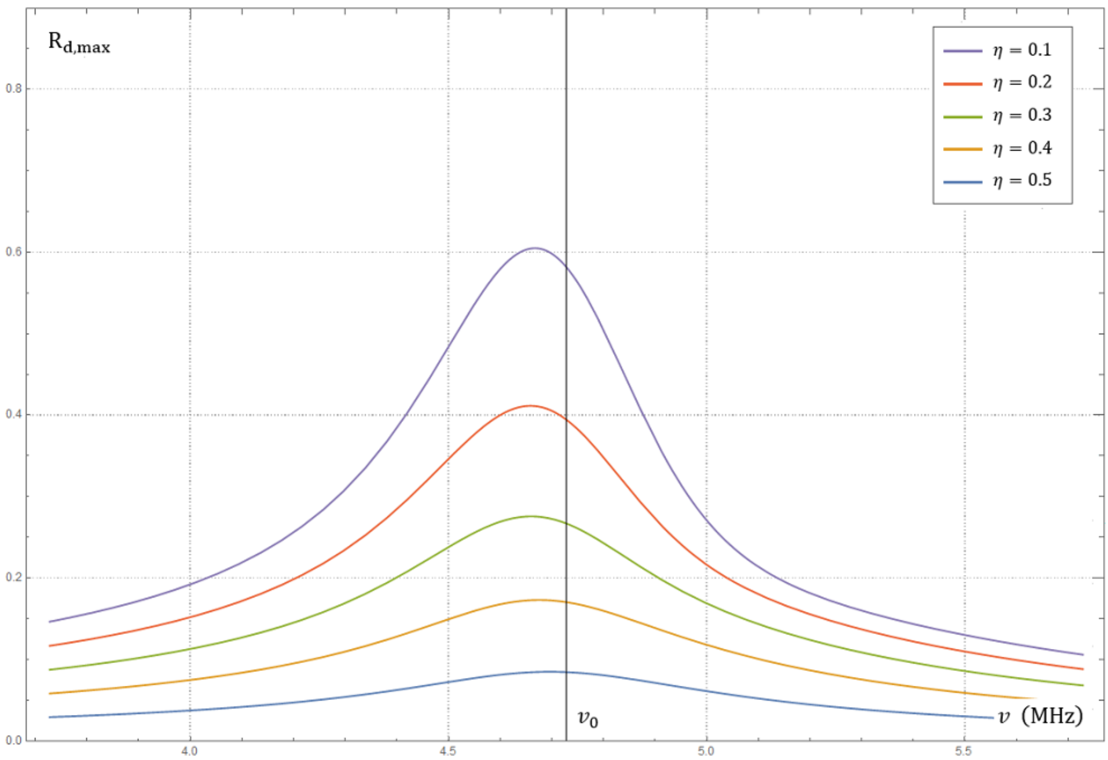

Fig.6.2 Response of a free bubble of initial radius R_0=1μm insonated by an external sinusoidal disturbance, immersed in a slightly compressible liquid

6.3 Encapsulated microbubbles

The response of encapsulated bubbles is examined next. As it was stated before, the compressibility effects add to the viscous damping of the problem. The response of an encapsulated bubble will be further attenuated due to the viscoelastic behavior of the membrane leading to lower amplitude values. The natural frequency of the problem is given by equation 3.2, and it is the same for all three constitutive laws. The general response, however, is heavily dependent on the law used, as it will be seen in the following paragraphs.

Plotting the amplitude of the fundamental mode of the oscillation up to the first approximation, equation 3.11, over the dimensional frequency yields the response curves of the bubble for different values of the disturbance amplitude. Three graphs have been produced one for each constitutive law used to describe the membrane.

6.3.1 Kelvin-Voight

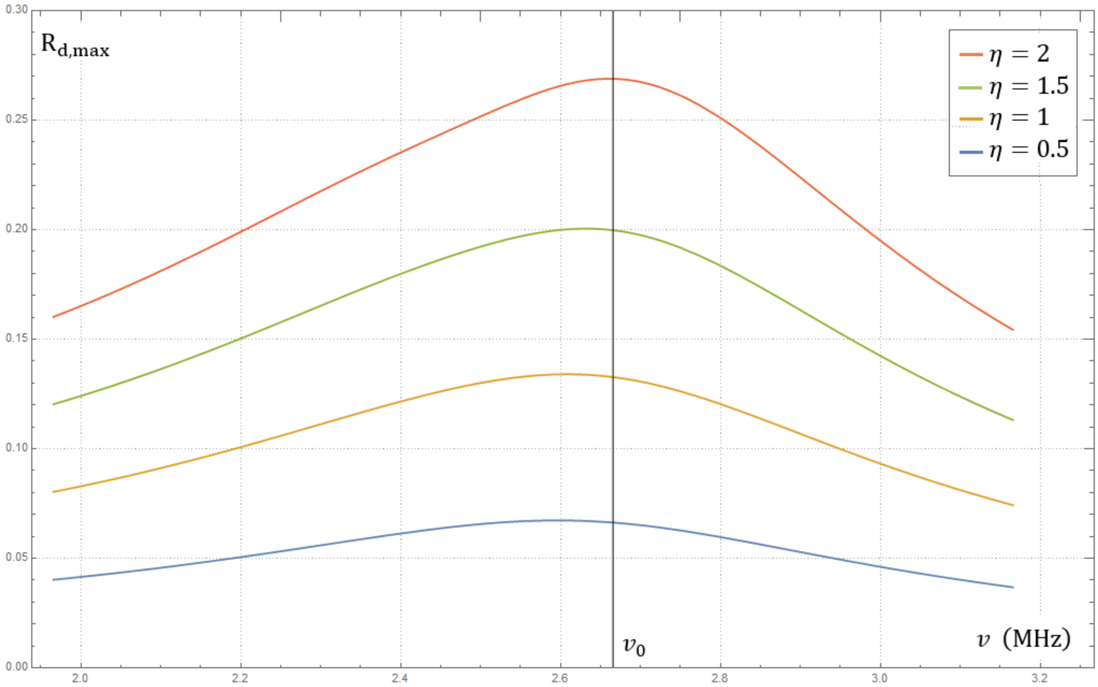

***Fig 6.3** Response of a KV membrane subject to a disturbance of increasing amplitude*

The Kelvin – Voight constitutive law corresponds to the linear representation of the membrane's stress strain behavior and it is applicable for small displacements. Even though it ignores the nonlinearity of the material, a shift ,in lower than the natural frequencies, is observed in the main resonance case and it is attributed solely to the increasing effect of inertia with nonlinearity which also decreases resonance frequency, Pelekasis Tsiglifis (2008) [15]. The KV shell applies a moderate resistance on the motion of the wall compared to the other two constitutive laws but high enough to attenuate the response dramatically when compared to the free bubble case. Due to the system's nonlinear behavior and the shift of frequency when a KV membrane is driven below resonance it can attain its resonance point with an increased amplitude while the initial radius of the shell remains the same. The driving regions above the resonant frequency, however, are not able to produce a strong response signal and a different choice of forcing frequency must be made in order attain the resonant state.

6.3.2 Mooney-Rivlin

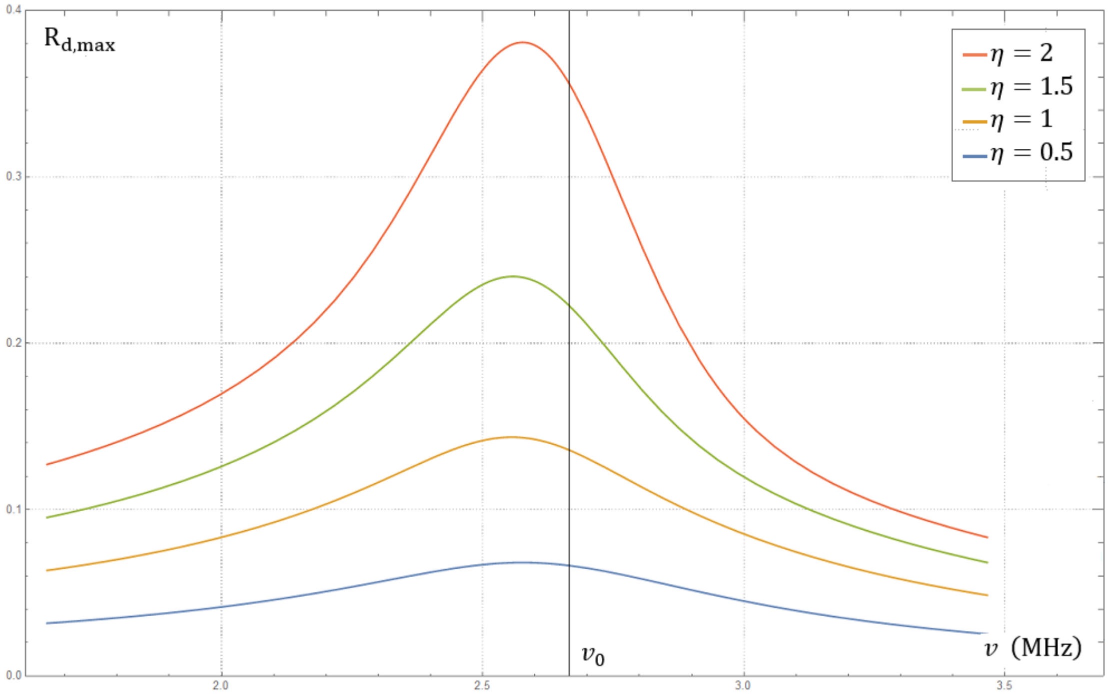

Fig 6.4 *Response of an MR membrane subject to a disturbance of increasing amplitude*

The Mooney – Rivlin constitutive law corresponds to a strain-softening nonlinear material, meaning a decreasing strain-stress slope is observed as deformation becomes larger. Parameter b which controls the softness of the membrane has been set to zero for the purposes of the present study. At first glance it is observed that the responses for every value of the external disturbance are moved to lower frequencies as it is to be expected from a strain-softening material. The restoring forces of the bubble become progressively weaker as the displacement from the equilibrium state grows to higher values. This leads to an enhancement of radial displacement and velocity that is larger than expected based solely on the amplitude of the acoustic disturbance. As the amplitude of the disturbance increases, resonance frequency decreases and the nonlinear resonance occurs at decreasing values. If the bubble is driven below resonance for small amplitudes of the disturbance it can hit its resonant point with a gradual increase of the external disturbance. However, when it is driven above resonance due to the strain-softening behavior of the shell and the shift to lower frequencies resonance cannot be achieved.

6.3.3 Skalak

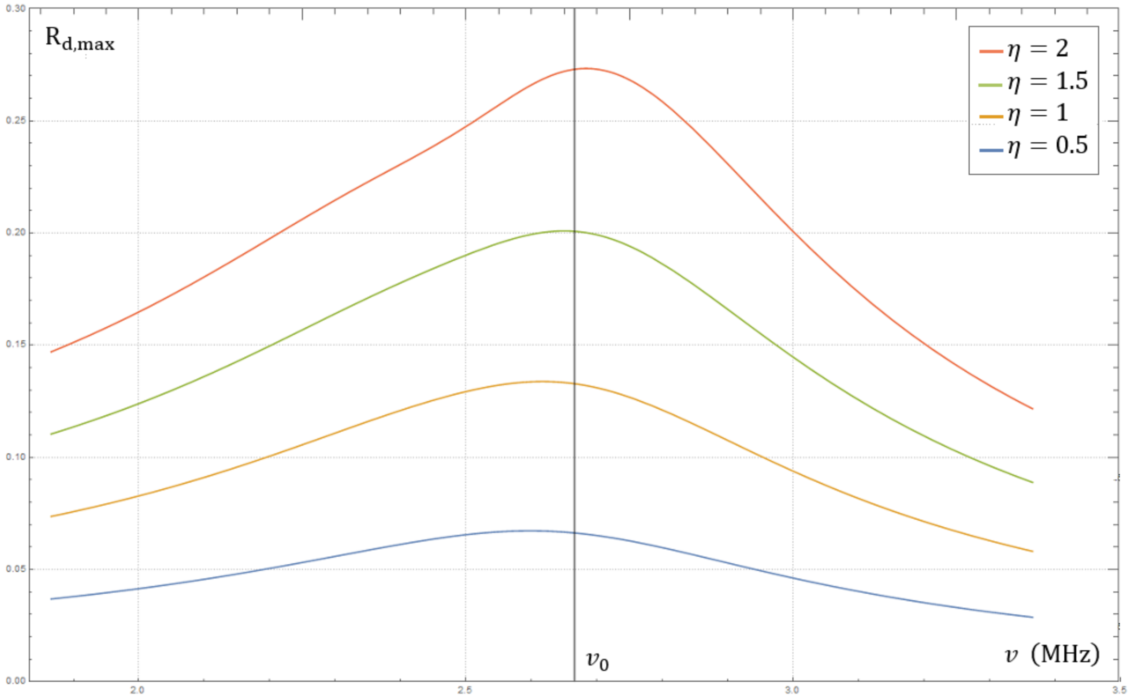

***Fig 6.5** Response of an SK membrane subject to a disturbance of increasing amplitude*

The Skalak constitutive law refers to a strain-hardening nonlinear material whose stress-strain slope increases as the displacement becomes bigger. Parameter C which denotes the area compressibility, i.e., stiffness for the shell material has been set to one for the present study, referring to a relatively strain-hardening material allowing for area compressibility phenomena on the membrane. It can be seen from the above graph that the resonance frequency of an SK material increases as the amplitude of the disturbance grows higher. The more intense the strain hardening behavior is the more evident is the shift. Hence, when a bubble is driven below the resonance frequency there is a possibility that main resonance will never occur due to this effect. However, if the bubble is driven at frequencies above the natural main resonance can be achieved, by increasing the amplitude of the disturbance, at higher frequencies if not achieved at lower values and a strong signal is observed while the nonlinear resonances occur. Due to the effective hardening of SK materials with increasing deformation it is observed that the membrane displacement and velocity at resonance values increase very mildly, as the higher the amplitude becomes owning to the additional resistance the SK membrane contributes to the system.

6.3.4 Remarks on the three constitutive laws.

From a qualitative point of view it can be deduced by comparing the peaks of the graphs that the resonant response is dependent on the law used to describe the membrane's material surrounding the bubble. Owning to its strain softening behavior an MR membrane is easier to expand and allows for larger deformations, whereas the opposite occurs for the strain-hardening case described by the SK constitutive law. The KV model which ignores any nonlinearities in the material's behavior lies in middle grounds and as it was stated, is valid for small deformations.

According to Barthes-Biesel et al. (2002)[12] et al in the asymptotic limit of small deformations all viscoelastic laws (KV, MR ,SK) reduce to Hooke's law which describes a linear stress-strain behavior. However, at large deformations the stress-strain relation is heavily dependent on the nature of the membrane constitutive law. This statement is in agreements with the results obtained in the present study. By comparing the graphs for each case, it can be observed that at lower values of the parameter η , controlling the amplitude of the imposed disturbance, the three laws tend to produce similar results regarding the magnitude of the amplitude as well as the value of the frequency where the nonlinear resonance occurs. However, at higher values of the pressure disturbance, the tree laws exhibit dissimilar behavior and adopt their characteristic properties.

In other words, SK membranes impose additional stiffness to the protective shell during expansion and consequently smaller excursions from sphericity, whereas the shell becomes softer during compression leading to larger excursions from sphericity. The overall effect during a period of the pulsation is a smaller effective bubble radius which generates a larger resonance frequency in comparison with the regime of infinitesimal disturbances. Thus, the resonant frequency obtained at higher disturbance amplitudes, where the nonlinear effects are experienced intensively, is larger than the KV and MR shells with the latter shell exhibiting the highest values of radial excursion during expansion due to the progressive softening of the membrane that allows for larger deformations.

Results regarding the resonant frequencies for each case exhibit a similar trend. For all three constitutive laws the natural frequency is the same, as it stems from the linear part of the equation of motion and thus the defining nonlinearities of each law do not contribute to its value. It is given by equation 3.2 and it increases as the elasticity of the material, described by the dimensionless number G, is increased. As the amplitude of the disturbance increases, the extend of the nonlinearity increases and resonance occurs in different values than the natural frequency. This is a known property of nonlinear oscillating systems and it is evident throughout the study. This deviation from linearity is observed as a decrease in resonant frequency for the KV and MR models, a slight one for the linear KV constitutive law and a much more noticeable for the MR describing the strain softening materials. However, when the SK constitutive law is employed to model the shell, a shift towards higher values is observed for the resonant frequency indicating a progressive stiffening of the membrane.

Once again, this effect is more evident as the amplitude of the disturbance grows higher and the nonlinear behavior of the materials exhibits its full effect. At lower values the three laws tend to produce similar results close to the linearized case as it is described by the KV constitutive law, a behavior in agreement with the Pelekasis and Tsiglifis, (2008) [15] simulations.

It should be lastly stressed that the main resonance frequency also depends on the initial radius of the bubble. The linear resonance frequency depends on the bubble size and it decreases as the latter grows higher. As a result, for strain-softening materials, whose resonance frequency leans towards lower values, when driven below resonance, a strong signal is acquired for smaller values of the external disturbance for higher initial radii. However, when a strain hardening material is put to the same test the possibility of resonance is eliminated since the resonant frequency increases with the amplitude of the disturbance. An excitation above resonance is needed to produce the opposite results regarding the two types of membranes.

6.3.5 Comparative presentation of the free and encapsulated bubbles

In this section we compare the responses of free and encapsulated bubbles. In both cases bubbles of initial radii $R_0 = 3\mu m$ immersed in the same host liquid, whose properties are stated in the beginning of the chapter, have been studied. The amplitude of the disturbance has been selected so that both responses are of the same magnitude for the results to be comparable and high enough so that the membrane of the encapsulated bubbles exhibits its full nonlinear behavior. For the free bubble case this corresponds to an external disturbance of amplitude $\eta = 0.1$, whereas for the encapsulated case a much higher value has been used to achieve similar responses, $\eta = 2$.

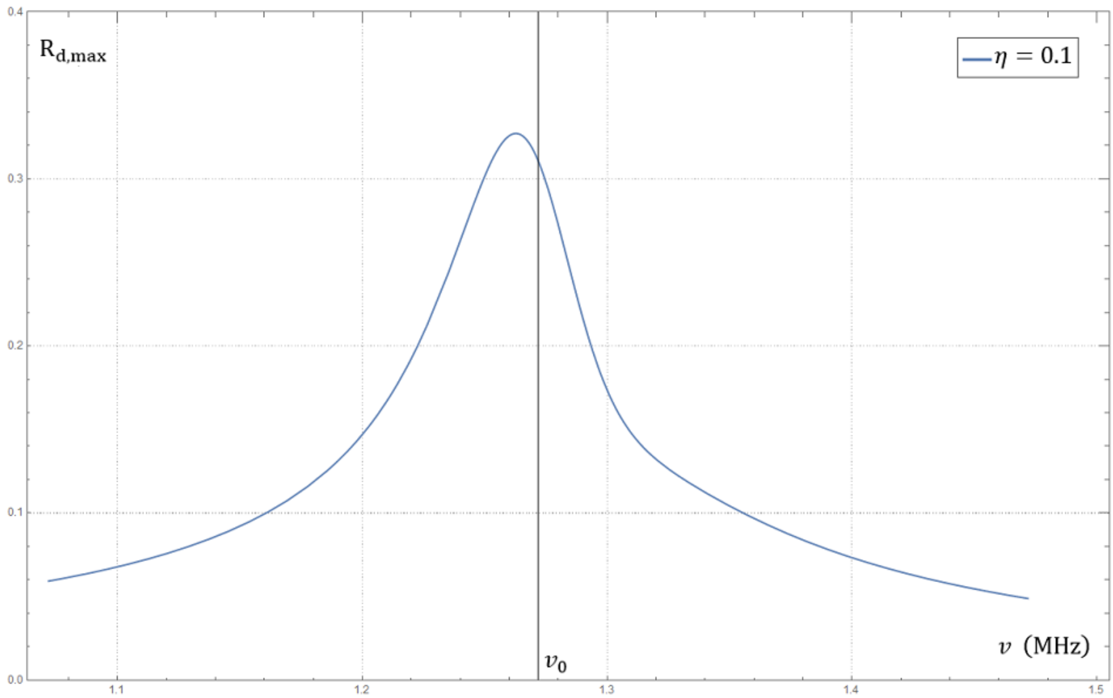

Fig 6.6 *Amplitude response of a free bubble immersed in a slightly compressible liquid.*

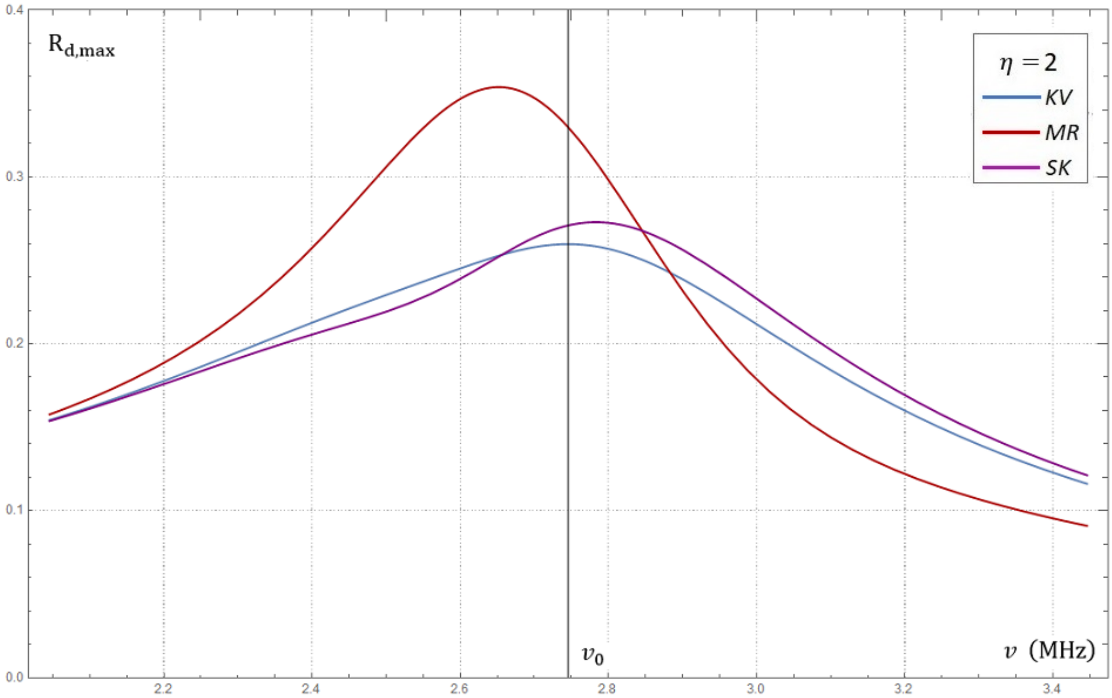

Fig 6.7 *Amplitude response of encapsulated bubbles described by KV, MR and SK constitutive laws immersed in a slightly compressible liquid*.

The free bubble eigenfrequency, given by equation 5.2, solely depends on the properties of the host liquid and the interface forming between it and the gas. For the encapsulated bubble an additional term rises in the eigenfrequency, equation 3.2, accounting for the membrane elasticity and, thus, it increases for more elastic materials without changing the liquid's properties. By comparing their expressions, it is evident that the natural frequency of the free bubble lies at much lower values.

A shift in resonance frequency is observed in both cases due to the heavily nonlinear nature of the governing equations of bubble dynamics. Resonance for free bubble systems occurs in lower than the natural frequencies, thus indicating a soft spring behavior where the softening on elongation overrides the hardening on compression Pelekasis and Tsiglifis, (2008) [15]. The exact value of frequency where the nonlinear resonance occurs depends on the amplitude of the oscillation and shifts to lower values the more intense the oscillations become. The same nonlinear behavior is observed in the encapsulated bubbles. However, the stress-strain relation of the material might impose additional nonlinear terms to the problem depending on the constitutive law used to describe it. For the KV case a shift in lower frequencies is observed and a much more noticeable one for an MR membrane owing to its strain-softening behavior. On the other hand, the strain-hardening membrane described by the SK constitutive law attains resonance at higher than the natural frequencies.

Regarding the amplitude of the response, it is evident from figures 6.6, 6.7 that it is heavily attenuated by the presence of an encapsulating membrane. Regardless of the constitutive law used to describe the material's viscoelastic behavior, a shell, which may be infinitesimally small compared to the initial radius of the bubble, provides a considerable amount of viscous damping to the problem. The stiffer the membrane is the higher the additional damping of the shell is. The response is so heavily diminished by the shell, that it was necessary the amplitude of the free response to be lower by a factor of ten to produce similar results even for the strain-softening case which allows for larger deformations.

6.3.6 Numerical results and comparison to analytical data obtained by the asymptotic expansion.

In the following paragraph a presentation of the results obtained by Pelekasis and Tsiglifis[15] in their respective study, concerning the free bubble as well as the encapsulated one obeying the KV, MR, SK constitutive laws is made . The numerical procedure followed, was exhibited in chapter 4. Figures of the study have been reproduced to illustrate the amplitude of the deviation from the equilibrium radius over the dimensional frequency to match the present study terminology, while ignoring any scattering effects for the pressure which played an important role in their paper. In both studies the same properties for the host liquid mentioned in the beginning of the chapter have been used and bubbles of the same initial radius have been employed for the results to be on common ground.

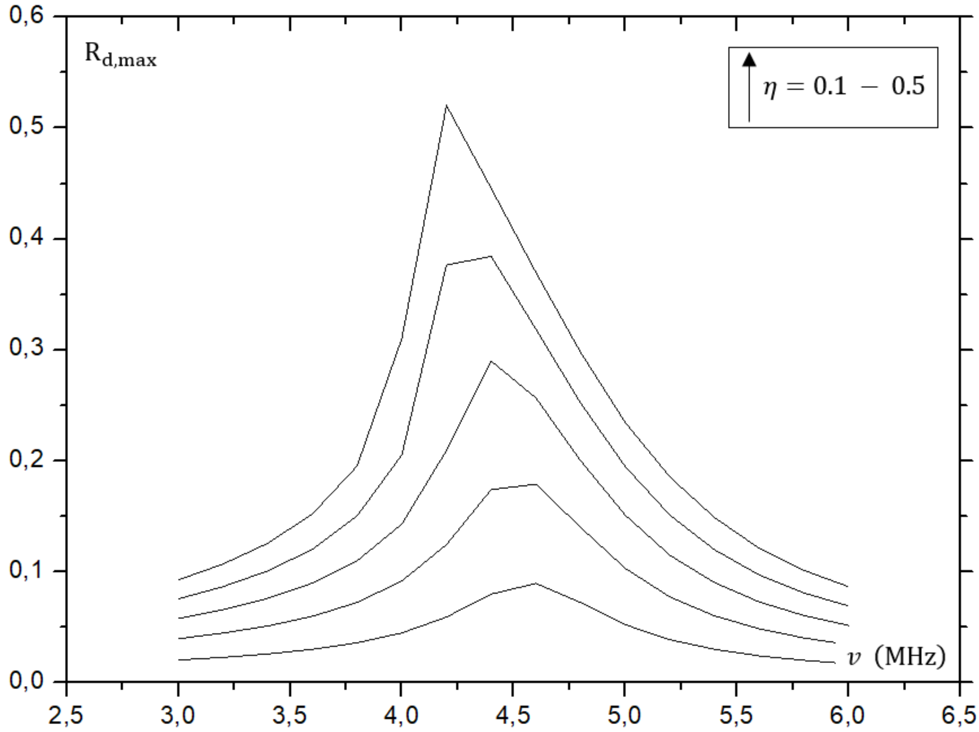

Fig 6.8 *Numerical response of a free bubble immersed in a slightly compressible liquid for increasing values of the disturbance amplitude*.

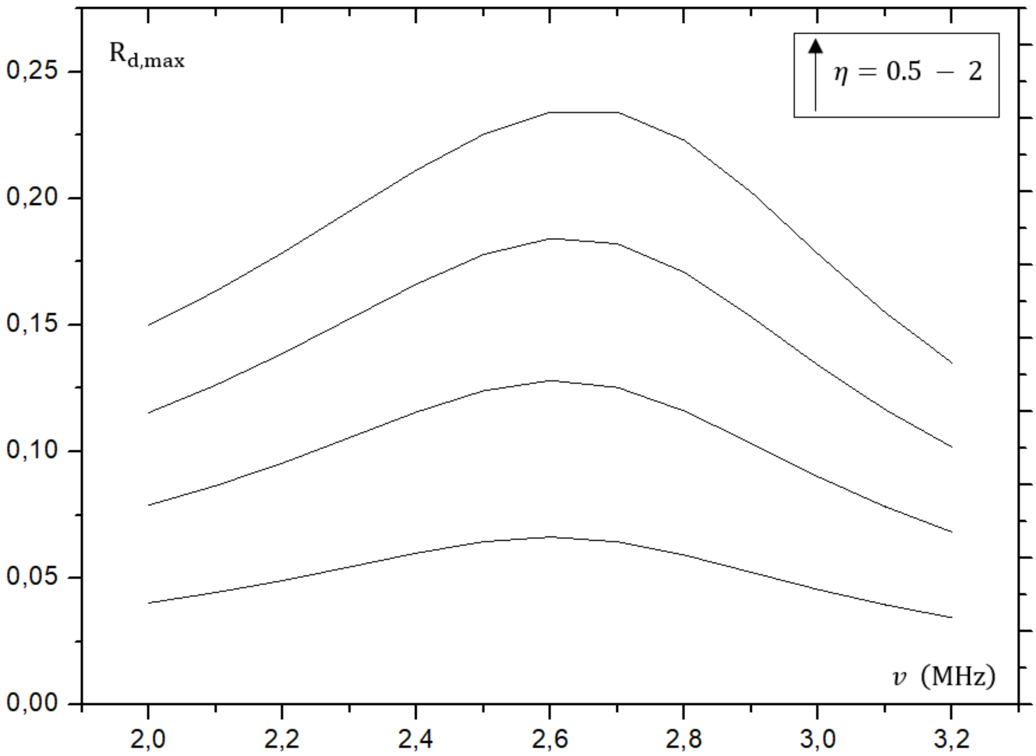

Fig 6.9 *Numerical response of a KV bubble immersed in a slightly compressible liquid for increasing values of the disturbance amplitude*.

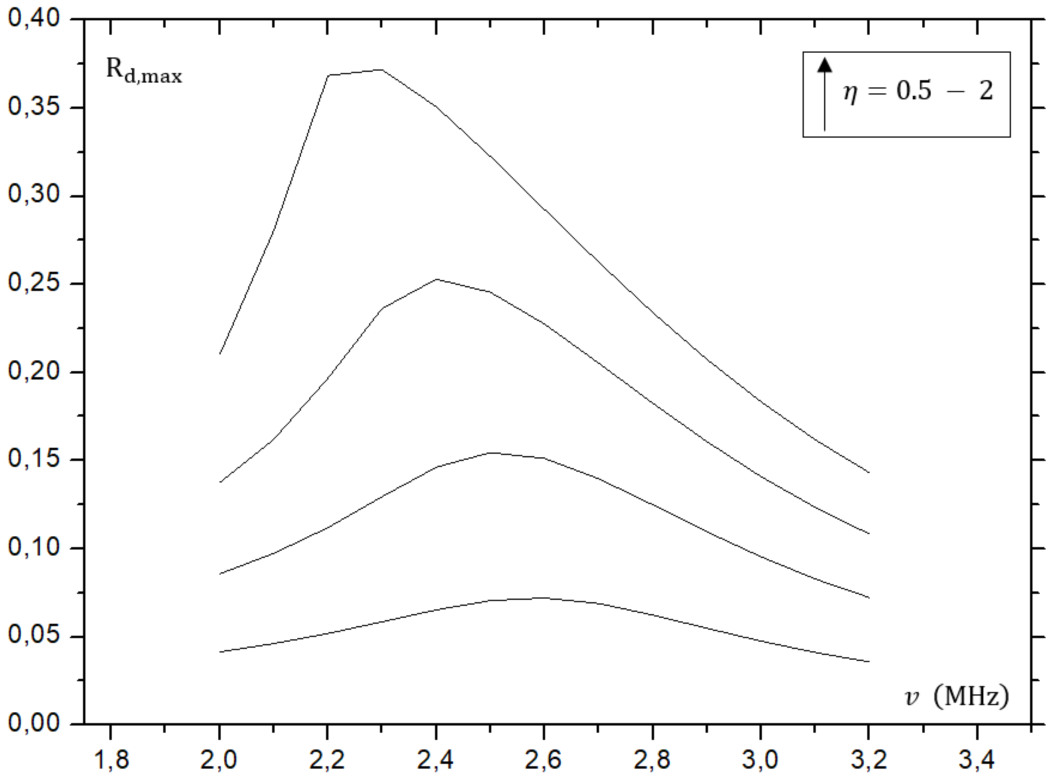

Fig 6.10 *Numerical response of an MR bubble immersed in a slightly compressible liquid for increasing values of the disturbance amplitude.*

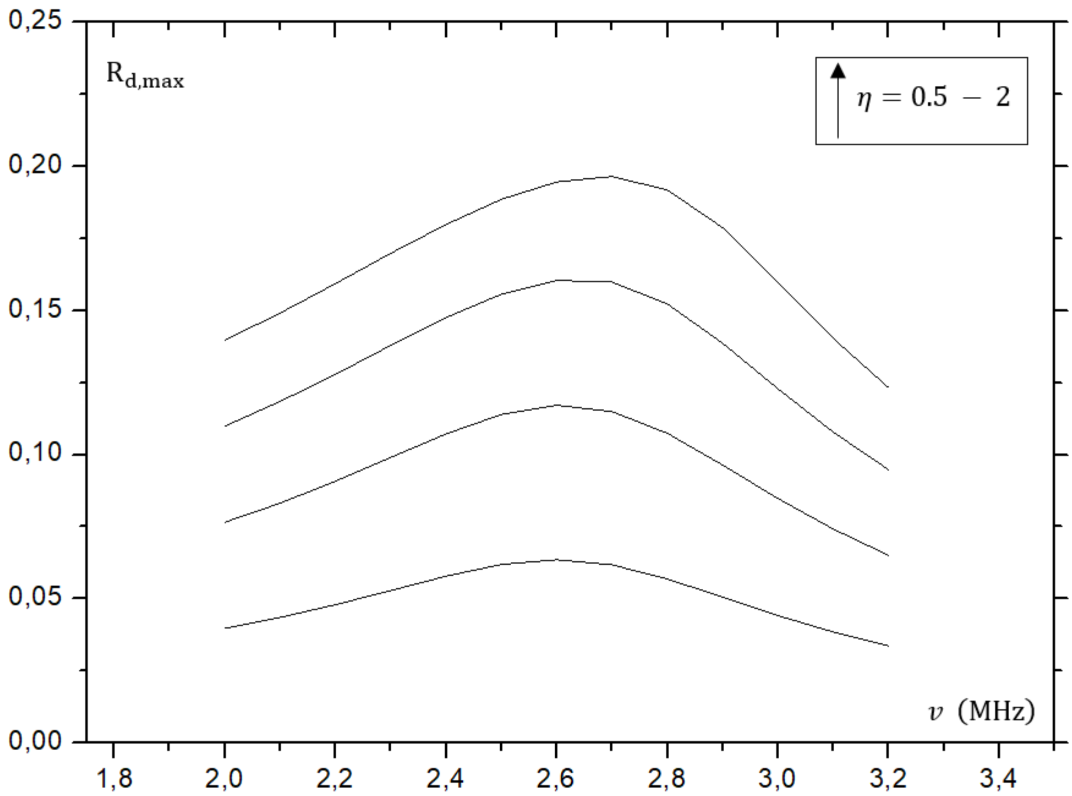

Fig 6.11 *Numerical response of an SK bubble immersed in a slightly compressible liquid for increasing values of the disturbance amplitude*.

Figure 6.8 is the numerical equivalent of figure 6.2 for the free bubble presented in the beginning of the present chapter while figures 6.9 ,6.10, 6.11 are the numerical equivalent of figures 6.3, 6.4 and 6.5 respectively, presented in the preceding paragraphs where the behavior of the material was investigated.

A more detailed comparison of the results obtained by both methods is presented in the following tables for each case.

<u>Free Gas Bubble</u> R_0 = 1μm, incompressible , V_0 = 4.72MHz

	Analytical		*Numerical*	
η	$\mathbf{R_{d,max}}$	$\mathbf{V_{res}}$ (MHz)	$\mathbf{R_{d,max}}$	$\mathbf{V_{res}}$ (MHz)
0.1	0.08506	4.68	0.08944	4.6
0.2	0.18017	4.66	0.17889	4.6
0.3	0.31048	4.66	0.28991	4.4
0.4	0.51463	4.67	0.38424	4.4
0.5	0.8398	4.68	0.52037	4.2

<u>Kelvin-Voight</u> R_0 = 3μm , v_0 = 2.66 MHz

	Analytical		*Numerical*	
η	$\mathbf{R_{d,max}}$	$\mathbf{V_{res}}$ (MHz)	$\mathbf{R_{d,max}}$	$\mathbf{V_{res}}$ (MHz)
0.5	0.06727	2.59	0.06634	2.6
1	0.13399	2.61	0.1281	2.6
1.5	0.20048	2.63	0.1843	2.6
2	0.26891	2.66	0.2314	2.7

<u>Mooney-Rivlin</u> R_0 = 3μm , v_0 = 2.66 MHz

	Analytical		*Numerical*	
η	$\mathbf{R_{d,max}}$	$\mathbf{V_{res}}$ (MHz)	$\mathbf{R_{d,max}}$	$\mathbf{V_{res}}$ (MHz)
0.5	0.06819	2.58	0.07212	2.6
1	0.14354	2.55	0.15464	2.5
1.5	0.24013	2.56	0.25921	2.4
2	0.38081	2.57	0.37183	2.3

<u>Skalak</u> R_0 = 3μm , v_0 = 2.66 MHz

	Analytical		*Numerical*	
η	$\mathbf{R_{d,max}}$	$\mathbf{V_{res}}$ (MHz)	$\mathbf{R_{d,max}}$	$\mathbf{V_{res}}$ (MHz)
0.5	0.06722	2.6	0.0636	2.6
1	0.13378	2.62	0.11715	2.6
1.5	0.20093	2.65	0.1605	2.6
2	0.27335	2.68	0.19652	2.7

Table 1 *Amplitude and resonance frequency comparison for analytically and numerically obtained results.*

Comparing results obtained in both studies, there seems to be a satisfactory agreement especially for the lower values of the parameter η which controls the amplitude of the disturbance. An overall overestimation of values is evident from Table 1 for increasing values of amplitude, where the results are compared side by side for each case. Regarding the resonance frequencies, the numerical results exhibit a wider range of values where the nonlinear resonance occurs while the analytical results tend to place the resonant value to a small range close to the natural frequency of the case studied.

The validity of an asymptotic analysis lies on nonlinear terms being relatively small. As the disturbance grows larger it imposes greater deformations to the bubble wall which leads to higher values of the amplitude. The nonlinearities present in the governing equations of bubble dynamics contain terms of acceleration, velocity and displacement of the bubble wall which grow larger as the external disturbance increases. So, as the nonlinear terms are described less accurately by small parameters the results obtained analytically tend to become less valid.

Comparing the graphs, a good agreement is found from a quantitative point of view. The method was able to capture the shift in frequencies of the nonlinear resonance for all the three constitutive laws and was able to describe to the strain-softening and strain hardening behavior of the nonlinear materials described by them, while the amplitudes of the bubble wall all lie in the same order of magnitude. However, when the numerical free bubble and, more noticeably, Mooney – Rivlin graphs are observed, a steeper slope appears when approaching the resonant point from lower frequencies for the higher values of the external disturbance which the analytical solution was not able to portray. This is due to the restricted range of resonant frequencies provided for these high values of sound amplitude by the asymptotic analysis employed for the present study. The near resonance case used, equation 3.4, describes the shift from the linear resonance frequency for small values of the parameter ε, thus any results obtained are restricted to small deviations.

Concluding, the divergence from the numerical results lies within acceptable limits. A more thorough study of the ordering of the small parameters involved in the problem could lead to even more accurate results even for the larger amplitude of the external disturbance while accounting for the remarks made in paragraph 5.2 regarding the order of the amplitude of the disturbance.

7 CONCLUSIONS – SUGGESTIONS FOR FURTHER STUDY

In the present study, the steady state of spherosymmetric volume oscillations of a gas bubble, free and encapsulated, in the main resonance area was investigated, through means of asymptotic expansions. The bubble was immersed in a Newtonian, slightly compressible liquid, free of any pre-stresses at equilibrium, when the full effects of viscosity were considered. To this end, the Keller-Miksis[6] model was employed to describe the oscillatory motion of the bubble's interface. For the encapsulated bubbles three constitutive laws were used, namely the Kelvin-Voight (KV), the Mooney-Rivlin and the Skalak (SK) models are used, pertaining to an almost linear for small displacements, strain-softening, and strain-hardening behavior of the material, respectively.

The asymptotic analysis followed the procedure that is suggested by Jordan and Smith[1] in their book. For the asymptotic scheme to hold valid results the nonlinear terms ought to be small. For this purpose, we assume that compressibility effects and viscous damping are small and more specifically of the first order. The bubble oscillates around its equilibrium radius and this deviation was also considered small. Lastly, the bubble was subject to an acoustic disturbance the amplitude of which was taken to be small, namely of the second order.

The amplitude of the fundamental oscillation of the bubble' deviation from the initial radius was extracted as a function of the detuning parameter, modified to be a function of the forcing frequency and plotted in frequency diagrams. Results concerning the free bubble case were compared to previous literature and numerical simulations. Despite discrepancies in the ordering of the disturbance amplitude, a quantitative agreement was found for relatively lower values of the sound amplitude. A shift of frequency towards lower values was observed for the nonlinear resonance indicating a soft spring behavior for the system. When the analytical results were compared to numerically obtained results by Pelekasis and Tsiglifis[15] the agreement was satisfactory for free and encapsulated bubbles.

The Kelvin-Voight constitutive law was used to describe an almost linear stress-strain behavior for small radial displacements. The response is heavily attenuated due to the elastic behavior of the membrane and a shift towards lower frequencies is observed for the non-linear resonance. The Mooney-Rivlin constitutive law is used to describe a strain softening stress-strain behavior due to the progressive thinning of the shell during expansion. Due to the strain softening nature of the membrane, as the disturbance amplitude increases, the bubble response increases disproportionately when compared to the linear predictions provided by the Kelvin-Voight model. Results have shown that, as the amplitude of the disturbance increases the nonlinear resonance occurs at lower frequencies, below the value of the linear resonance frequency. The deviation from the initial radius is larger during expansion and smaller during compression leading to a smaller effective radius during the span of one period of motion for Kelvin - Voight and Mooney - Rivlin membranes. However, due to the strain softening nature of the Mooney - Rivlin membranes the effective radius is larger and a more noticeable shift in frequencies is observed. Lastly, the Skalak constitutive law was used to model the strain-hardening behavior of the shell due to the almost area incompressible nature of the membrane. Unlike the two previous laws SK membranes exhibit larger excursions from sphericity during compression and smaller during expansion resulting to a smaller effective radius during a period and a shift towards higher frequencies was observed with an increasing amplitude. Due to the strain hardening nature of the shell, the attenuation of the amplitude was more noticeable with as the disturbance grew larger. On a comparative scale, the Mooney-Rivlin membranes give rise to the highest response amplitudes, the Skalak membranes the lowest while the Kelvin-Voight model predictions lie on middle grounds.

The results obtained analytically were compared to numerically attained values for the amplitude and resonance frequency. Regarding the amplitude values, a satisfactory agreement was found especially for lower values of the external disturbance. With more intense forcing a slight overestimation was observed was observed for the Kelvin-Voight and Mooney-Rivlin models and a more noticeable one for the Skalak law. The values of the resonance frequency were generally close to the numerical ones, especially for the smaller values of the sound amplitude. For the free bubble and the MR membrane, as the disturbance increases, the asymptotic expansion tends to produce results retaining the characteristic decrease of the frequency but contained to a smaller range of values around the linear resonance frequency.

It was pointed out that a better agreement of results was expected for smaller values of the acoustic disturbance amplitude. As the amplitude grows higher, the deformations applied in the bubble become larger and the nonlinear parameters cannot be described by small parameters properly. The ordering of the variables involved, as it was presented in paragraph 3.1.2, breaks down and the results obtained become less valid as the disturbance becomes more and more intense.

It can be deduced by the present study that a lot of phenomena occur during the oscillations in the presence of an acoustic disturbance even when they are considered spherosymmetric and the only direction investigated is the radial one. On the contrary a bubble can execute volume, shape oscillations or a combination of both, which makes the problem a lot more complicated. Constitutive laws used to describe the membrane's behavior play an important role to the response. Further study could implement more cases regarding the values of parameters b and C denoting the membrane softness for the Mooney-Rivlin law and membrane compressibility for the Skalak law respectively. As it was stated in paragraph 2.2.2 parameter b lies in the range between 0 and 1 and the lower its value is the softer the membrane. Parameter C dictates area incompressibility and the higher its value is the more intense the strain hardening behavior of the shell is. Different kinds of material can be examined by simply choosing different values for the above parameters. Pelekasis and Tsiglifis, (2011)[16] performed such an analysis in the context of forced oscillations of a free bubble with a viscoelastic coating and predicted eigenfrequencies of shape modes as well as stability criteria. Moreover, the latter analytical solution can be extended to include residual stresses on the shell and investigate how they affect the bubble response. Such a study is in progress and associates residual stresses with the compression only effect; Vlachomitrou & Pelekasis (2021). The effect of scattering of pressure on the shell of the bubble could also be studied once an expression of the bubble instantaneous radius is obtained. Usually, such oscillatory motions of bubbles occur in ultrasound medical procedures where the host liquid is not infinite. A very important subject for future study pertains to the development of a theoretical/numerical approach to study the effect nearby boundaries in the flow on the backscattered pressure. Existing studies focus on standard free bubbles, Oguz & Prosperetti (1998)[10], or study coated microbubbles in the absence of nearby boundaries, Efthymiou et al. (2017)[18]. In a more recent study Vlachomitrou and Pelekasis, (2021)[21],[22], introduced the effect of an interacting solid boundary without focusing on the resulting resonance frequencies. Such a preliminary study was conducted in the context of the Ms Thesis by Chrysostomidis (2018)[19] using the boundary element methodology and an extended study is in progress in order to account for shape oscillations using the finite element methodology, Vlachomitrou & Pelekasis (2021)[23],[24]. Lastly, a more detailed approach regarding the ordering of parameters and the asymptotic scheme used could be done in a way that the approximate analytical solution provides more accurate results for higher values of the imposed disturbance.

8 REFERENCES

[1] D. W. Jordan and P. Smith, "Nonlinear ordinary differential equations".

[2] Skalak, R., Tozeren, A., Zarda, R. P., and Chien, S. (1973). "Strain energy function of red blood cell membranes," Biophys. J. 13, 245–280.

[3] Andrea Prosperetti, (1974). "Nonlinear oscillations of gas bubbles in liquids: steady-state solutions" J. Acoust. Soc. Am. 56, No.3.

[4] Werner Lauterborn, (1976). "Numerical investigation of nonlinear oscillations of gas bubbles in liquids", J. Acoust. Soc. Am. 59, No.2.

[5] L. Samek, (1980). "Nonlinear oscillations of gas bubbles in liquids" Czech. J. Phys. B30.

[6] Joseph B. Keller and Michael Miksis, (1980). "Bubble oscillations of large amplitude" J. Acoust. Soc. Am. 68, 628–633.

[7] A. Prosperetti and A. Lezzi, (1986). "Bubble dynamics in a compressible liquid. Part 1 . First-order theory" J. Fluid Mech. 168, 457–478.

[8] Charles C. Church, (1995). "The effects of an elastic solid surface layer on the radial pulsations of gas bubbles" J. Acoust. Soc. Am. 97, 1510–1521.

[9] Peter J. A. Frinking and Nico De Jong, (1998). "Acoustic modeling of shell-encapsulated gas bubbles" ,Ultrasound Med. Biol. 24 523–533.

[10] Oguz & Prosperetti (1998) The natural frequency of oscillation of free bubbles in tubes", J. Acoust. Soc. Am. 103 (6), June 1998

[11] Damir B. Khismatullin and Ali Nadim, (2002). "Radial oscillations of encapsulated microbubbles in viscoelastic liquids", Phys. Fluids 14, 3534–3556.

[12] Dominique Barthes-Biesel, Anna Diaz and Emmanuelle Dhenin, (2002). "Effect of constitutive laws for two-dimensional membranes on flow-induced capsule deformation", J. Fluid Mech. 460, 211–222.

[13] Nikos A. Pelekasis, Alexandra Gaki, Alexander Doinikov, John A. Tsamopulos, (2004). “Secondary Bjerknes forces between two bubbles and the phenomenon of acoustic streamers”, J. Fluid Mech. 500, 313–347.

[14] P. Marmottant, S. van der Meer, M. Emmer, M. Versluis, N. de Jong, S. Hilgenfeldt, and D. Lohse, (2005). J. Acoust. Soc. Am. 118(6), 3499–3505.

[15] Kostas Tsiglifis and Nikos A. Pelekasis, (2008). “Nonlinear radial oscillations of encapsulated microbubbles subject to ultrasound: The effect of membrane constitutive law”, J. Acoust. Soc. Am. 123, 4059-4070.

[16] Kostas Tsiglifis and Nikos A. Pelekasis, (2011). “Parametric stability and dynamic buckling of an encapsulated microbubble subject to acoustic disturbances”, : Phys. Fluids 23, 012102

[17] Yanjun Gong, Mario Cabodi, and Tyrone M. Porter, (2014). “Acoustic investigation of pressure-dependent resonance and shell elasticity of lipid-coated monodisperse microbubbles” , Applied Physics Letters 104.

[18] K. Efthymiou, N. Pelekasis, M. B. Butler, D. H. Thomas, and V. Sboros, (2017). “The effect of resonance on transient microbubble acoustic response: Experimental observations and numerical simulations”, J. Acoust. Soc. Am. 143

[19] A. Chrysostomidis (2018) “Study of the resonance frequencies of coated microbubbles pulsating in cylindrical tube via the boundary element methodology”, Diploma Thesis submitted to the University of Thessaly in partial fulfillment of the requirements for an Ms Thesis.

[20] J. Naude, F. Méndez, C. Yepes, M. Navarrete, R.F. Cienfuegos-Pelaes, F. Moumtadi, (2020). “Frequency response curves for a Mooney-Rivlin hyperelastic microbubble oscillating as a contrast agent in an acoustic pressure field”, Ultrasonics 107.

[21] Maria Vlachomitrou, Nikos Pelekasis, (2021). “Numerical study of the interaction between a pulsating coated microbubble and a rigid wall. I. Translational motion”, Physical Review Fluids 6

[22] Maria Vlachomitrou, Nikos Pelekasis, (2021). “Numerical study of the interaction between a pulsating coated microbubble and a rigid wall. II. Trapped pulsation”, Physical Review Fluids 6

[23] Maria Vlachomitrou & Nikos Pelekasis (2021) “Microbubble pulsations in the vicinity of a solid boundary: Effect of residual stresses on the phenomenon of acoustic streamers”, In preparation.

[24] Maria Vlachomitrou & Nikos Pelekasis (2021) “Coated microbubbles pulsating in a tube: Effect of tube size and sound amplitude on the resonance frequency”, In preparation.